In this study, we examined the involvement of interaction between integrins and penton base RGD motifs in subgroup B Ad35 vector-mediated transduction in human bone marrow-derived CD34$^+$ cells and human leukemia cell line K562 cells, both of which have been shown to be highly susceptible to Ad35 vectors.[15,23,24] Human bone marrow-derived CD34$^+$ cells are an important target for gene therapy, because the CD34$^+$ cells are a fraction that contains hematopoietic stem cells. We found that inhibition of the interaction between integrins and penton base RGD motifs did not alter total amounts of cell-associated vector DNA of Ad35 vectors at 4 or 37 °C; however, it significantly reduced the transduction efficiencies of Ad35 vectors, suggesting that interaction between integrins and penton base RGD motifs is largely involved with Ad35 vector-mediated transduction, probably in postinternalization steps.

Results

Several types of integrins are expressed on human bone marrow-derived CD34$^+$ cells and K562 cells

First, we performed flow cytometric analysis to examine which types of integrins are expressed on human bone marrow-derived CD34$^+$ cells and K562 cells. Flowcytometric analysis demonstrated that the CD34$^+$ cells and K562 cells both expressed high levels of integrins α_5 (95%; CD34$^+$ cells, 100%; K562 cells) and β_2 (99%; CD34$^+$ cells, 86%; K562 cells) (Figure 1). Integrins α_4, α_6 and β_1 were also expressed in the CD34$^+$ cells, but hardly detected in K562 cells. Integrins $\alpha_v\beta_3$ and $\alpha_v\beta_5$, which are well known as second receptors for Ad5 vectors,[3,4] were expressed in low levels in both cells ($\alpha_v\beta_3$; 13 and 20% in CD34$^+$ cells and K562 cells, respectively; $\alpha_v\beta_5$; 2 and 17% in CD34$^+$ cells and K562 cells, respectively).

Divalent cations are required for Ad35 vector-mediated transduction

Next, to examine involvement of integrins in Ad35 vector-mediated transduction, the hematopoietic cells were transduced with Ad35 vectors in the presence of EDTA or divalent cations. The affinity between integrins and their ligands is regulated by divalent cations.[25–27] Notably, Mn^{2+} is reported to largely promote the binding of ligands to integrins. Transduction efficiencies of an Ad35 vector expressing an enhanced green fluorescence protein (GFP) (Ad35GFP) in K562 cells were significantly reduced in the presence of EDTA (Figure 2a). Treatment with 5 mM EDTA decreased GFP expression by 80%. On the other hand, Mn^{2+} significantly increased the transduction efficiencies of Ad35GFP in K562 cells, while exposure to Mg^{2+} or Ca^{2+} did not affect the transduction efficiencies of Ad35GFP (Figure 2b). These results suggest that integrins are involved with Ad35 vector infection. Transduction experiments using the CD34$^+$ cells were also tried; however, pretreatments with EDTA or divalent cations largely reduced the viability of the CD34$^+$ cells (data not shown).

To investigate the mechanisms of EDTA-mediated decrease and the Mn^{2+}-mediated increase in transduction efficiencies of Ad35 vectors, cellular binding and uptake of Ad35GFP in the presence of EDTA or Mn^{2+} was assessed by real-time PCR. Exposure to 5 mM EDTA or Mn^{2+} did not increase the total amounts of Ad35 vector genome associated with K562 cells at 4 °C 1.5 h following infection, indicating that cellular binding of Ad35GFP is not affected by divalent cations (Figure 3). In addition, the cells treated with EDTA or Mn^{2+} also showed no change in the amounts of cell-associated Ad35 vector DNA at 37 °C (the sum of cellular binding and uptake of Ad35GFP). These results suggest that postinternalization steps in Ad35 vector-mediated transduction are affected by EDTA and Mn^{2+}.

Penton base RGD motifs are involved with Ad35 vector-mediated transduction

To examine whether the RGD motifs in the Ad35 penton base are involved with Ad35 vector-mediated transduction in the CD34$^+$ cells and K562 cells, the cells were transduced with Ad35GFP in the presence of synthetic RGD peptide. Transduction with Ad35GFP was significantly suppressed by the RGD peptide in a dose-dependent fashion in the human CD34$^+$ cells and K562 cells (Figure 4). The GFP expression levels by Ad35GFP in the CD34$^+$ cells and K562 cells were respectively

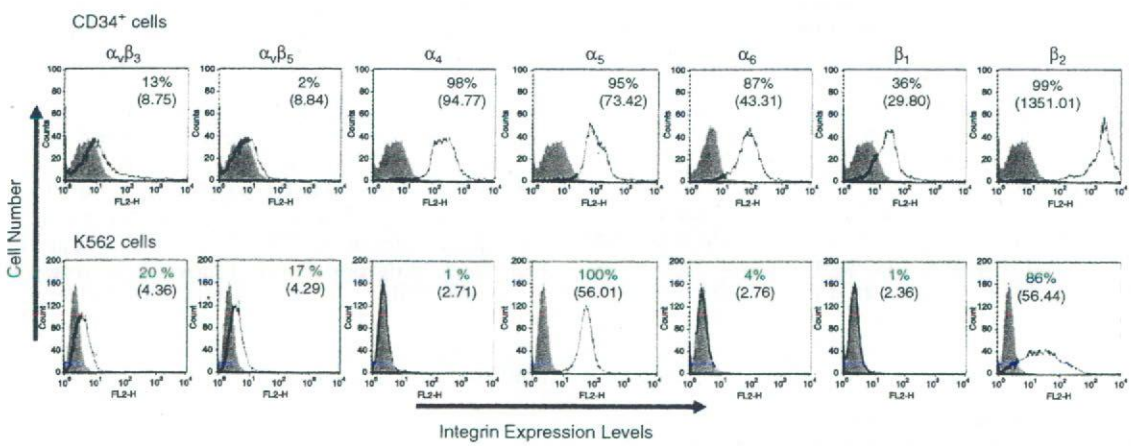

Figure 1 Flow cytometric profiles of integrin expressions on human bone marrow-derived CD34$^+$ cells and K562 cells. The cells were stained with monoclonal anti-integrin antibodies, followed by a phycoerythrin-labeled secondary antibody, and subsequently analyzed by a flow cytometry (thick line). As a negative control, cells were incubated with an isotype control antibody (shaded histogram). Percentages of positive cells (and mean fluorescence intensities) are shown by number in the upper right-hand corner of each profile.

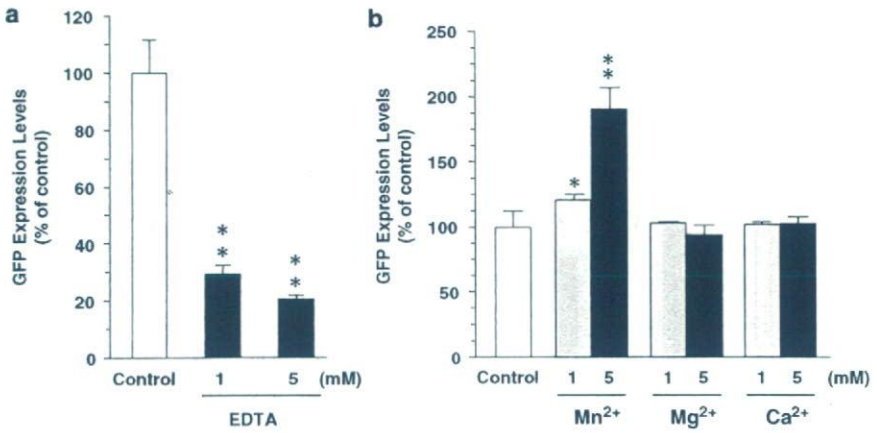

Figure 2 Effects of divalent cations on Ad35 vector-mediated transduction. (**a**) Ad35GFP-mediated transduction in the presence of EDTA. K562 cells were transduced with Ad35GFP at 1000 VP per cell for 1.5 h in the presence of EDTA at the indicated concentrations. GFP expression levels were measured using flow cytometry 48 h after transduction. The GFP expression levels (mean fluorescence intensity; MFI) in the absence of EDTA (control) and the mock-infected cells were 107.6 and 2.4, respectively. (**b**) Ad35GFP-mediated transduction in the presence of Mn^{2+}, Mg^{2+} or Ca^{2+} ions. K562 cells were preincubated in TBS buffers containing $MnCl_2$, $MgCl_2$ or $CaCl_2$ at indicated concentrations for 30 min and then transduced with Ad35GFP at 1000 VP per cell. The transduction experiments were performed as described above. The GFP expression level (MFI) in TBS buffer (control) and the mock-infected cells were 119.3 and 2.3, respectively. The data were normalized to the GFP expression levels (MFI) in K562 cells, which were preincubated in TBS buffer prior to transduction (control). Data are expressed as means ± s.d. ($n = 3$ or 4). $^*P < 0.05$, $^{**}P < 0.001$ in comparison with the control. TBS, Tris-buffered saline.

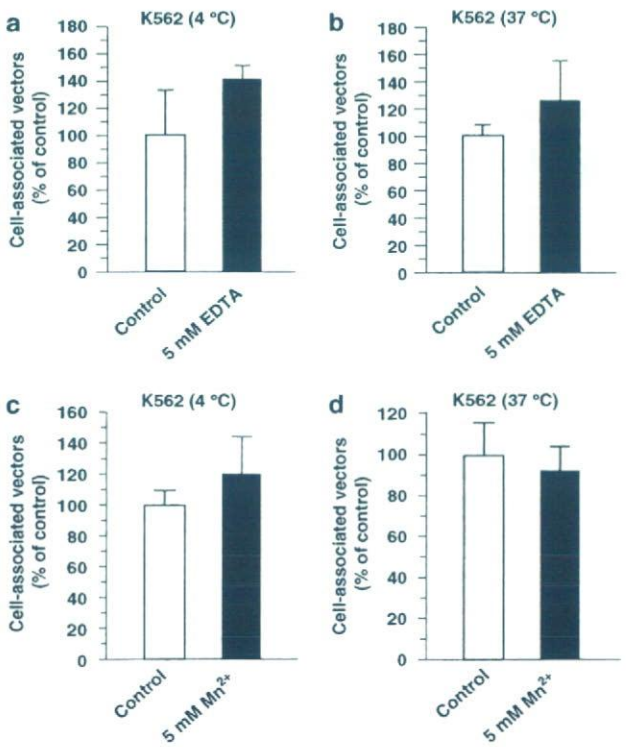

Figure 3 Effects of divalent cations on cellular binding and uptake of Ad35 vectors in K562 cells. K562 cells were incubated with Ad35GFP in the presence of 5 mM EDTA (**a**, **b**) or 5 mM Mn^{2+} (**c**, **d**) as described in Figure 2. After incubation, the cells were washed and total DNA, including Ad vector DNA, was recovered. The vector copy number was quantified using real-time PCR. The data were normalized to the vector copy number when transduced with Ad35GFP in Tris-buffered saline buffer. Data are expressed as means ± s.d. ($n = 4$). GFP, green fluorescence protein.

decreased by 57 and 24% in the presence of 200 μg ml^{-1} of the RGD peptide, compared with the presence of the control RGE peptide.

Next, to clarify why coincubation with the RGD peptide decreases the transduction efficiencies of Ad35 vectors, we evaluated cellular binding and uptake of Ad35 vectors in the presence of the RGD peptide. As shown in Figure 5, the RGD peptide did not decrease the total amounts of cell-associated vector DNA of Ad35GFP at 4 or 37 °C in the $CD34^+$ cells and K562 cells, suggesting that the interaction between integrins and penton base RGD motifs are crucial for Ad35 vector-mediated transduction; however, this interaction would not be largely involved with the cellular binding or uptake of Ad35 vectors in the $CD34^+$ cells and K562 cells.

Mutation of penton RGD motifs in Ad35 vectors significantly reduces the transduction activity of Ad35 vectors

To further examine the involvement of penton RGD motifs with Ad35 vector-mediated transduction, we constructed Ad35 vectors containing the RGE sequence instead of RGD in the penton base (D343E) (Ad35RGE-GFP) or a deletion of the RGD motifs in the penton base (Ad35ΔRGD-GFP) (Table 1). Final yields of Ad35RGE-GFP and Ad35ΔRGD-GFP were comparable to those of Ad35GFP (data not shown). The $CD34^+$ cells exhibited approximately 80% reduction in GFP expression following transduction with Ad35RGE-GFP and Ad35ΔRGD-GFP at 6000 vector particles (VP) per cell (Figure 6a). In K562 cells, Ad35RGE-GFP and Ad35ΔRGD-GFP mediated approximately 35% reduced GFP expression compared with Ad35GFP at 3000 VP per cell (Figure 6b). Transduction with each Ad35 vector at lower doses resulted in similar transduction profiles to those shown here in the $CD34^+$ cells and K562 cells (data not shown),

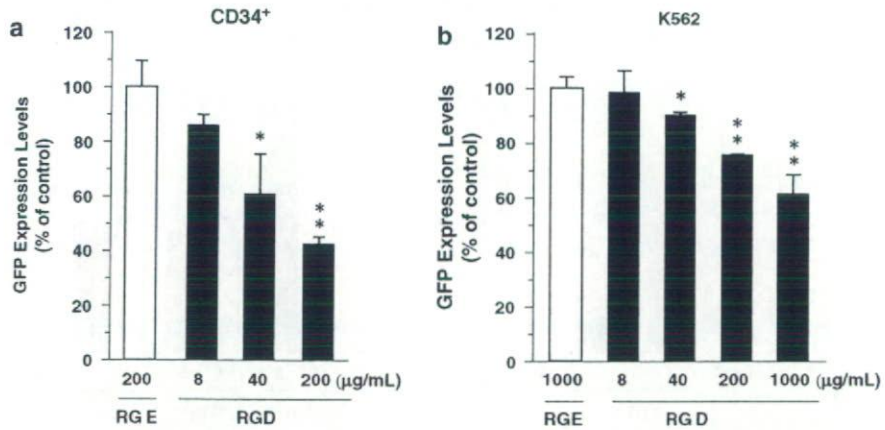

Figure 4 Inhibition of Ad35 vector-mediated transduction by synthetic RGD peptide. Human CD34+ cells (**a**) and K562 cells (**b**) were transduced with Ad35GFP at 3000 VP per cell for 3 h (human CD34+ cells) or at 1000 VP per cell for 1 h (K562 cells) at 37 °C in the presence of RGD peptides. GFP expression levels were measured 48 h after transduction by flow cytometry. Data were normalized to the GFP expression levels (MFI) in the presence of control RGE peptide. The GFP expression levels (MFI) in the presence of control RGE peptide (CD34+ cells; 200 μg ml^{-1}, K562 cells; 1000 μg ml^{-1}) were 198.2 (CD34+ cells) and 748.9 (K562 cells). The GFP expression levels (MFI) in the mock-infected cells were 2.3 (CD34+ cells) and 2.9 (K562 cells). The Data are expressed as means ± s.d. ($n = 3$). *$P < 0.05$, **$P < 0.001$ in comparison with control RGE peptide. MFI, mean fluorescence intensity; RGD, Arg-Gly-Asp.

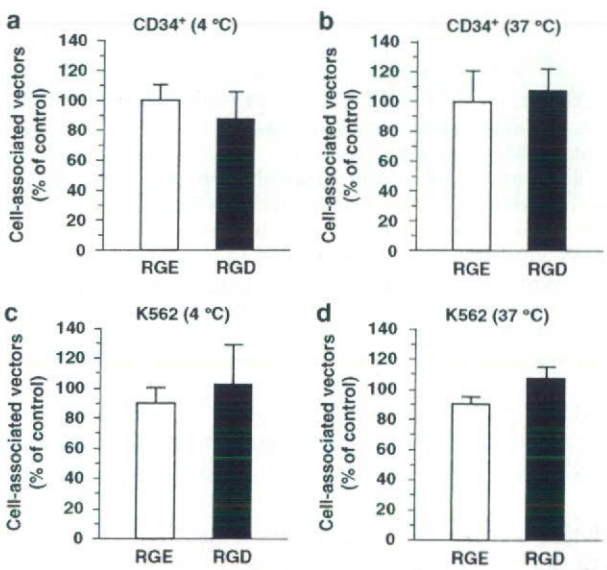

Figure 5 Cellular binding and uptake of Ad35GFP in the presence of RGD peptide. Human CD34+ cells (**a**, **b**) and K562 cells (**c**, **d**) were incubated with Ad35GFP in the presence of RGD peptide (200 μg ml^{-1}) as described in Figure 4. After incubation, the cells were washed, and total DNA, including Ad vector DNA, was recovered. The vector copy number was quantified using real-time PCR. The data were normalized to the vector copy number of Ad35GFP in the presence of control RGE peptide. Data are expressed as mean ± s.d. ($n = 4$). GFP, green fluorescence protein; RGD, Arg-Gly-Asp; RGE, Arg-Gly-Glu.

suggesting that the transduction efficiencies of the Ad35 vectors at these doses would not be saturated. Apparent toxicities were not observed in the cells after transduction at these doses (data not shown). These results indicate that penton base RGD motifs are largely involved with Ad35 vector-mediated transduction in both cells.

Table 1 Mutation in the penton base of Ad35 vectors

Ad35 vectors	*Amino-acid sequence of penton base*
Ad35GFP (conventional Ad35)	—NAGEV**RGD**NFAPT—
Ad35RGE-GFP (an amino acid substitution)	—NAGEV**RGE**NFAPT—
Ad35ΔRGD-GFP (deletion of RGD motif)	—NAGEV - - - - - - - - - NFAPT—

Abbreviations: Ad, adenovirus; GFP, green fluorescence protein; RGD, Arg-Gly-Asp.

Next, we compared the cellular binding and uptake of Ad35GFP, Ad35RGE-GFP and Ad35ΔRGD-GFP in the CD34+ cells and K562 cells by real-time PCR analysis to examine why the mutation of penton base RGD motifs decreased the transduction efficiencies. We found that 3 h (CD34+ cells) or 1.5 h (K562 cells) following infection, the Ad35 vector genome levels associated with both cells were comparable to those of Ad35GFP, Ad35RGE-GFP and Ad35ΔRGD-GFP at 4 and 37 °C (Figure 7), although the amount of Ad35ΔRGD-GFP associated with the CD34+ cells at 37 °C was significantly higher than those of the other vectors. These results indicate that penton base RGD motifs play an important role in postinternalization steps.

Integrins $\alpha_v\beta_3$, $\alpha_v\beta_5$ and α_5 are involved with Ad35 vector infection

To determine which types of integrins participate in Ad35 vector infection in the CD34+ cells and K562 cells, we performed an infection-blocking experiment using several anti-integrin antibodies. Among the several anti-integrin antibodies, incubation with anti-$\alpha_v\beta_3$ antibody significantly reduced the GFP expression level by 41% in the CD34+ cells (Figure 8a). The other types of anti-integrin antibodies did not inhibit Ad35 vector-mediated

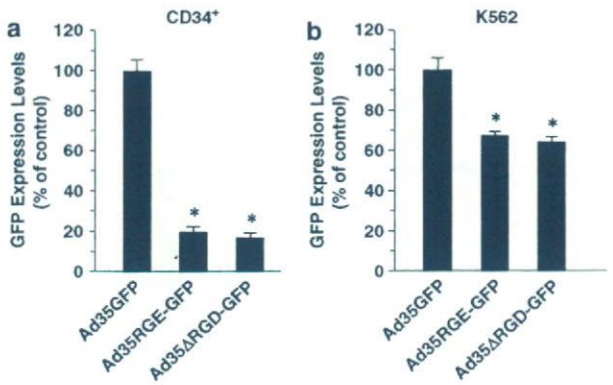

Figure 6 Effects of modification of penton RGD motifs on transduction efficiencies of Ad35 vectors. Human CD34⁺ cells (**a**) and K562 cells (**b**) were transduced with Ad35GFP, Ad35RGE-GFP and Ad35ΔRGD-GFP at 6000 VP per cell for 6 h (human CD34⁺ cells) or at 3000 VP per cell for 1.5 h (K562 cells) at 37 °C. GFP expression levels (MFI) were measured 48 h after transduction using flow cytometry. The GFP expression levels of Ad35GFP in the CD34⁺ cells and K562 cells were 432.4 and 3232.7, respectively. The GFP expression levels in the mock-infected cells were 3.2 (CD34⁺ cells) and 3.3 (K562 cells). The data were normalized to the GFP expression levels by Ad35GFP. Data are expressed as means ± s.d. ($n = 3$). *$P < 0.001$ in comparison with Ad35GFP. GFP, green fluorescence protein; MFI, mean fluorescence intensity; RGD, Arg-Gly-Asp.

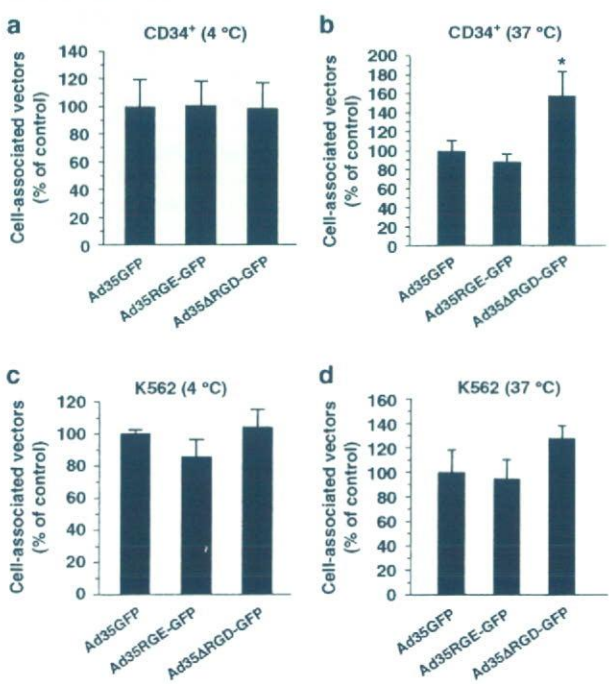

Figure 7 Effects of modification of penton RGD motifs on cellular binding and uptake of Ad35 vectors. Human CD34⁺ cells (**a**, **b**) and K562 cells (**c**, **d**) were incubated with Ad35GFP, Ad35RGE-GFP and Ad35ΔRGD-GFP as described in Figure 6 at 4 or 37 °C. After incubation, the cells were washed five times with ice-cold phosphate-buffered saline, and total DNA, including the Ad vector DNA, was extracted. The vector copy numbers were quantified by real-time PCR. The data were normalized to the vector copy number of Ad35GFP. Data are expressed as means ± s.d. ($n = 4$). *$P < 0.05$ in comparison with Ad35GFP. GFP, green fluorescence protein; RGD, Arg-Gly-Asp.

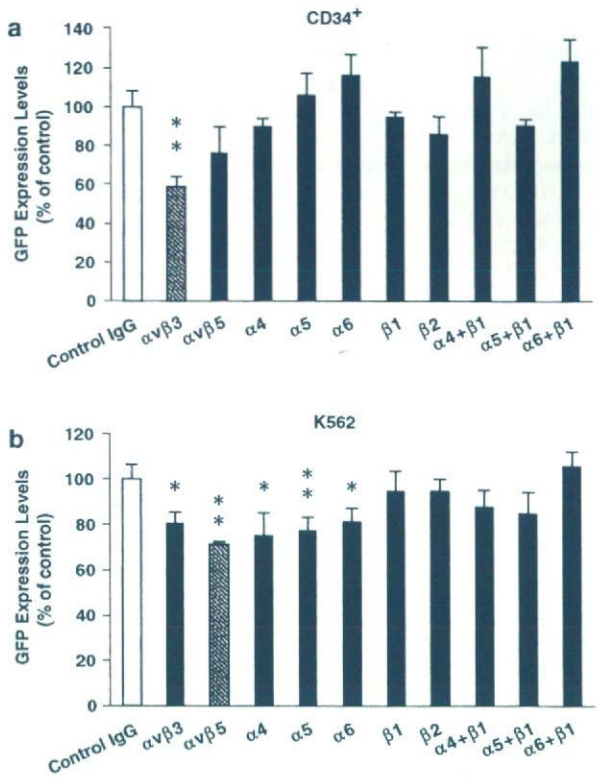

Figure 8 Inhibition of Ad35 vector-mediated transduction by monoclonal anti-integrin antibodies. Human CD34⁺ cells (**a**) and K562 cells (**b**) were transduced with Ad35GFP at 3000 VP per cell for 3 h (human CD34⁺ cells) or at 300 VP per cell for 0.5 h (K562 cells). GFP expression levels were measured 48 h after transduction using flow cytometry. The GFP expression levels (MFI) in the presence of control IgG were 427.0 (CD34⁺ cells) and 24.9 (K562 cells). The GFP expression levels in the mock-infected cells were 2.8 (CD34⁺ cells) and 2.7 (K562 cells). The data were normalized to the GFP expression levels (MFI) in human CD34⁺ cells and K562 cells in the presence of control mouse IgG. Data are expressed as means ± s.d. ($n = 3$). *$P < 0.05$, **$P < 0.01$ in comparison with control IgG. GFP, green fluorescence protein; IgG, immunoglobulin G; MFI, mean fluorescence intensity

transduction in the CD34⁺ cells. In K562 cells, Ad35GFP showed 20, 30 and 22% reduced levels of GFP expression in the presence of anti-$\alpha_v\beta_3$, -$\alpha_v\beta_5$ and -α_5 antibodies, respectively (Figure 8b). Pretreatment with anti-α_4 and anti-α_6 antibodies in K562 cells also significantly decreased GFP expression by Ad35GFP, in spite of undetectable expression levels of these integrins in K562 cells (see Figure 1). These results indicate that the integrins described above are involved with Ad35 vector-mediated transduction in the CD34⁺ cells or K562 cells.

Discussion

The goal of this study was to evaluate the involvement of interaction between penton base RGD motifs and integrins on the cell surface with Ad35 vector-mediated transduction in human hematopoietic cells. To this end, we performed transduction with Ad35 vectors in hematopoietic cells in the presence of EDTA, divalent

cations and RGD peptide. Ad35 vectors with a mutation in the penton base were constructed, and transduction properties of the mutant Ad35 vectors were examined. Furthermore, Ad35 vectors transduced hematopoietic cells in the presence of several types of anti-integrin antibodies.

The interaction of penton base RGD motifs with α_v integrins is well known to facilitate the internalization of Ad5 vectors via clathrin-mediated endocytosis.[28] Several types of integrins, such as $\alpha_v\beta_3$, $\alpha_v\beta_5$ and $\alpha_v\beta_1$, mediate efficient transduction with Ad5 vectors.[2–6] The structures of the Ad5 fiber and penton base allow easy access of penton base RGD motifs to integrins on the cell surface. Ad5 possess a long (22 β-repeats), and flexible fiber shaft.[29,30] The RGD-containing hypervariable loop of the Ad5 penton base is longer than those of other serotypes,[20,21] and protrudes above the penton base.[31] In contrast, the fiber shaft of Ad35 is short (7 β-repeats).[30] The hypervariable loop of the Ad35 penton base is 19 amino-acid shorter than that of Ad5. These properties of Ad35 suggest that the RGD motifs in the Ad35 penton base might be less easily associated with integrins on the cell surface. The present study indicates that the interaction of penton base RGD motifs in Ad35 with integrins is not largely involved with the cellular binding and uptake of Ad35. Segerman *et al.*[32] and Tuve *et al.*[33] also demonstrated that the presence of divalent cations, which increases the affinity of integrins to their ligands, did not affect the cellular binding of subgroup B Ads. Properties of CD46 also contribute to the lack of necessity of interaction between penton base RGD motifs and integrins for uptake of Ad35. Gaggar *et al.*[11] suggested that CD46 is not only an attachment receptor, but also a receptor for internalization of Ad35. The cytoplasmic tail of CD46 possesses a signal sequence for endocytosis.[34]

The experimental method used in this study does not allow exact evaluation of the internalized Ad35 vector copy numbers, because the amounts of the vector copy numbers at 37 °C contains both the virus particles attached on the cell surface and those truly internalized into the cells. However, it is unlikely that the amounts of Ad35 vector particles bound on the cell surface are dramatically different between 4 and 37 °C, because CD46 expression levels on the cell surface did not decrease at the Ad35 vector dose used in this study (data not shown). Therefore, we can roughly estimate that the amounts of the internalized Ad35 vector particles are not dramatically different in the presence or absence of EDTA, Mn^{2+} or the RGD peptide, assuming that the amounts of the Ad35 vector particles bound on the cell surface at both temperatures are the same.

However, interaction of penton base RGD motifs with integrins might facilitate the internalization rates of CD46-utilizing Ad vector particles into cells, especially shortly after virus infection. Deletion of penton base RGD motifs in chimeric Ad5 vectors containing the Ad35 fiber knob showed 15-min delays in the postinfection uptake of the vectors.[35] Ad serotype 41, which lacks an RGD motif on the penton base, undergoes delayed uptake in A549 cells.[21]

On the other hand, inhibition of interaction between the RGD motifs and integrins significantly decreased the transduction activity of Ad35 vectors, indicating that binding of the RGD motifs to integrins is largely involved with the transduction process of Ad35 vectors. Our group also confirmed that fiber-substituted Ad5 vectors bearing the fiber shaft and knob of Ad35 with deletion of penton base RGD motifs showed reduced transduction efficiencies compared with the parent fiber-substituted Ad5 vectors (data not shown). Shayakhmetov *et al.*[35] also demonstrated that mutation of penton base RGD motifs in chimeric Ad5 vectors containing the fiber knob of Ad35 significantly decreased the transduction efficiencies. These results indicate that penton base RGD motifs are important for transduction with not only subgroup B Ad vectors, but also CD46-utilizing chimeric Ad5 vectors. It remains unclear which process is facilitated by interaction between Ad35 penton base RGD motifs and integrins. However, the present study revealed that interaction of the RGD motifs with integrins did not significantly enhance cellular binding and uptake of Ad35, suggesting that postinternalization steps, such as escape from endosomes/lysosomes, would be accelerated by the interactions. This hypothesis is supported by the study by Shayakhmetov *et al.*,[35] which demonstrated that deletion of penton RGD motifs in chimeric Ad5 vectors possessing the fiber knob of Ad35 decreased escape from the endosomes/lysosomes. The interaction of $\alpha_v\beta_5$ integrins with penton RGD motifs was reported to enhance the escape of Ad5 from endosomes.[4]

Although significant decreases in the transduction activities were found in Ad35 vectors with a mutation of the RGD motifs, Ad5 vectors with deletion of penton base RGD motifs exhibited approximately comparable levels of transgene expression in CAR-positive cells with normal Ad5 vectors.[35,36] The difference between Ad5 and Ad35 vectors in their need for penton base RGD motifs for efficient transduction might be due to the difference in their ability to escape from endosomes. Ad5 vectors are released from endosomes immediately after endocytosis; in contrast, chimeric Ad5 vectors possessing the fiber knob of Ad35, which are supposed to show similar intracellular trafficking to Ad35 vectors, remained longer in late endosomes/lysosomes than conventional Ad5 vectors.[37]

Blocking studies using anti-integrin antibodies revealed that integrins involved with Ad35 vector infection are $\alpha_v\beta_3$ in the $CD34^+$ cells and $\alpha_v\beta_3$, $\alpha_v\beta_5$ and α_5 in K562 cells (anti-α_4 and anti-α_6 antibodies showed statistically significant inhibition in Ad35 vector-mediated transduction; however, expressions of α_4 and α_6 integrins are below detectable levels, as commented in the result section). Before the experiments, we had speculated that $\alpha_5\beta_1$ integrin was mainly involved with Ad35 vector-mediated transduction, because human bone marrow $CD34^+$ cells expressed integrins α_5 and β_1. In addition, the affinity of ligands to integrins is influenced by the amino acid following the RGD sequence while the RGDN (Arg-Gly-Asp-Asn) sequence, which is contained in the Ad35 penton base, has a high affinity for $\alpha_5\beta_1$ integrin.[38] However, the efficiencies of Ad35GFP transduction did not decrease in the presence of anti-α_5 or anti-β_1 antibodies in the $CD34^+$ cells, although preincubation with anti-α_5 antibody reduced transduction of Ad35GFP in K562 cells. It remains unclear why $\alpha_5\beta_1$ integrin is not involved with Ad35 vector infection in the $CD34^+$ cells. In addition, only the anti-$\alpha_v\beta_3$ antibody inhibited transduction with Ad35 vectors in the $CD34^+$ cells, and anti-integrin antibodies used in this study showed low levels of inhibition in both cells. Other types

of integrins which were not tested in this study, or unknown receptor(s), might be involved with Ad35 infection.

In summary, we demonstrated that the interaction between penton base RGD motifs and integrins are important for Ad35 vector-mediated transduction in hematopoietic cells. The results of our study contribute to a better understanding of the mechanism of Ad35 vector-mediated transduction and may offer valuable information for the development of more efficient Ad vectors.

Materials and methods

Cells and antibodies

Human bone marrow-derived $CD34^+$ cells (Cambrex Bio Science Inc., Walkersville, MD, USA) were recovered from the frozen stock 16–18 h before transduction, and suspended in StemSpan 2000 containing the cytokine cocktail StemSpan CC100 (human Flt-3 ligand (100 ng ml^{-1}), human stem cell factor (100 ng ml^{-1}), human interleukin-3 (20 ng ml^{-1}) and human interleukin-6 (20 ng ml^{-1})) (StemCell Technologies Inc., Vancouver, BC, Canada). K562 cells (human chronic myelogeneous leukemia from blast crisis) were maintained in RPMI 1640 medium supplemented with 10% fetal calf serum. Purified function-blocking monoclonal antibodies to integrins $\alpha_v\beta_3$ (LM609), $\alpha_v\beta_5$ (P1F6), α_5 (P1D6), β_1 (P4C10) and β_2 (P4H9-A11) were purchased from Chemicon International (Temecula, CA, USA). Monoclonal antibodies to integrin α_4 (HP2/1) and α_6 (GoH3) were obtained from Immunotech (Marseille, France) and R&D Systems Europe (Abingdon, UK), respectively.

Plasmids

Ad35 vector plasmid pAdMS18 was constructed as follows. The *Sbf*I/*Asc*I fragment of pAdMS1,[15] which is the left end of the Ad35 genome (1–7930 bp), was ligated with the *Sbf*I/*Asc*I fragment of pFS2,[15] resulting in pFS2-Ad35-12. pFS2-Ad35-12 was cut by *Sna*BI and *Pac*I, and ligated with oligonucleotides 1 (5′-TAACTATAACGGTC CTAAGGTAGCGA*ATTTAAAT***ATCTATGTCGGGTGCG GAGAAAGAGGTAATGAAATGGCA**AT-3′) and 2 (5′-T **GCCATTTCATTACCTCTTTCTCCGCACCCGACATAG AT***ATTTAAAT***T**CGCTACCTTAGGACCGTTATAGTTA-3′) (I-*Ceu*I, *Swa*I and PI-*Sce*I recognition sequences are noted by underlining, italics and bold, respectively), resulting in pFS2-Ad35-13, which contains I-*Ceu*I, *Swa*I and PI-*Sce*I sites in the E1 deletion site of the Ad35 genome. The I-*Ceu*I/*Asc*I fragments of pFS2-Ad35-13 and pAdMS4[23] were ligated, resulting in pAdMS18. pAdMS18 has I-*Ceu*I, *Swa*I and PI-*Sce*I sites in the E1 deletion region (ΔE1:450–2912 bp).

Vector plasmids pAdMS19 and pAdMS20, which were used to generate Ad35 vectors containing an amino-acid substitution in the penton RGD sequence (D343E) or a deletion of the RGD motif in the penton base, respectively, were constructed using the following procedures. pFS5-Ad35-2 was constructed by ligation of the *Asc*I/*Eco*RI fragment (7930–21 944 bp) of the Ad35 genome and the *Asc*I/*Eco*RI fragment of pFS5. pFS5 was constructed by ligation of *Xba*I/*Sac*I-digested pHM5[39] with the oligonucleotides containing the multicloning sites. A shuttle plasmid pFS4, which contains the multicloning site, *Pme*I/*Asc*I/*Nhe*I/*Bst*1107I/*Csp*45I/*Pac*I/*Not*I, was digested with *Sph*I/*Csp*45I and ligated with the *Sph*I/*Csp*45I fragment of pFS5-Ad35-2, resulting in pFS4-Ad35-1. pFS4 was constructed by ligation of *Sph*I/*Sal*I-digested pHM5 with oligonucleotides containing the multicloning site. pFS4-Ad35-2, which has the Ad35 genome (14 409–15 544 bp), was constructed by ligation of *Bst*1107I/*Csp*45I fragments of pFS4-Ad35-1 and pFS4. Then, pFS4-Ad35-2 was cut by *Pvu*II and *Pst*I, and ligated with oligonucleotides 3 (5′-CTGCTGCA GAAGCTAAGGCAAACATAGTTGCCAGCGACTCTAC AAGGGTTGCTAACGCTGGAGAGGTCAGAGGAGAG AATTTTGCGCCAACACCTGTTCCGACTGCA-3′) and 4 (5′-GTCGGAACAGGTGTTGGCGCAAAATTCTCTCCTC TGACCTCTCCAGCGTTAGCAACCCTTGTAGAGTCGC TGGCAACTATGTTTGCCTTAGCTTCTGCAGCAG-3′) (the RGE sequence is underlined), resulting in pFS4-Ad35-5. pFS4-Ad35-5 was digested with *Sph*I/*Pvu*II and ligated with the *Sph*I/*Pvu*II fragment of pFS4-Ad35-1, resulting in pFS4-Ad35-6. pFS4-Ad35-7, which was constructed by ligation of the I-*Ceu*I/*Blp*I fragment of pFS5-Ad35-2 and I-*Ceu*I/*Blp*I-digested pFS4-Ad35-6, were cut by *Sgr*AI/*Pac*I and ligated with the *Sgr*AI/*Pac*I fragment of pFS5-Ad35-2, resulting in pFS4-Ad35-9. Finally, pAdMS19 was constructed by homologous recombination of the *Asc*I/*Pac*I fragment of pFS4-Ad35-9 with *Bst*1107I-digested pAdMS18 in *Escherichia coli* BJ5183. pAdMS20 was similarly constructed using oligonucleotides 5 (5′-CTGCTGCAGAAGCTAAGGCA AACATAGTTGCCAGCGACTCTACAAGGGTTGCTAA CGCTGGAGAGGTCAATTTTGCGCCAACACCTGTTCC GACTGCA-3′) and 6 (5′-GTCGGAACAGGTGTTGGCG CAAAATTGACCTCTCCAGCGTTAGCAACCCTTGTA GAGTCGCTGGCAACTATGTTTGCCTTAGCTTCTGCA GCAG-3′).

Virus

The Ad35 vectors were prepared by means of an improved *in vitro* ligation method described previously.[23,39,40] GFP-expressing Ad35 vector plasmids (pAdMS18CA-GFP, pAdMS19CA-GFP and pAdMS20CA-GFP) were constructed by ligation of I-*Ceu*I/PI-*Sce*I-digested pAdMS18, pAdMS19 and pAdMS20, respectively, and I-*Ceu*I/PI-*Sce*I-digested pHMCA5-GFP. pHMCA5-GFP was constructed by insertion of the GFP gene, which was derived from pEGFP-N1 (Clontech, Mountain View, CA, USA) into pHMCA5.[41]

To generate the virus, pAdMS18CA-GFP, pAdMS19-CA-GFP and pAdMS20CA-GFP were digested with *Sbf*I and purified by phenol–chloroform extraction and ethanol precipitation. Linearized plasmids were transfected into 293E1B cells[42] with SuperFect (Qiagen, Valencia, CA, USA) according to the manufacturer's instructions. Determination of virus particle titers was accomplished spectrophotometrically by the method of Maizel *et al*.[43]

Flow cytometric analysis of integrin expressions

Human $CD34^+$ cells and K562 cells suspended in staining buffer (phosphate-buffered saline buffer containing 1% bovine serum albumin) were incubated with mouse anti-human integrin $\alpha_v\beta_3$, $\alpha_v\beta_5$, α_4, α_5, α_6, β_1 and β_2 antibodies for 1 h. Subsequently, the cells were reacted with phycoerythrin-labeled secondary anti-mouse IgG antibody (Pharmingen, San Diego, CA, USA). After washing

with the staining buffer, the stained cells (10^4 cells) were analyzed using FACSCalibur and CellQuest software (Becton Dickinson, Tokyo, Japan).

Transduction experiments

Human $CD34^+$ cells and K562 cells were seeded at 1×10^4 cells per well into a 96-well plate. The cells were transduced with Ad35GFP, Ad35RGE-GFP or Ad35ΔRGD-GFP at 6000 VP per cell for 6 h ($CD34^+$ cells) or 3000 VP per cell for 1.5 h (K562 cells). After a 48 h culture period, GFP expression levels were measured using flow cytometry as described above.

To examine the effects of divalent cations on Ad35 vector-mediated transduction, K562 cells were preincubated in Tris-buffered saline buffer containing $MnCl_2$, $MgCl_2$ or $CaCl_2$ at indicated concentrations for 30 min at 4 °C prior to transduction. Subsequently, the cells were transduced with Ad35GFP at 1000 VP per cell for 1.5 h at 37 °C. After a 1.5 h incubation, the cells were washed and resuspended in a fresh medium. GFP expression levels were measured using flow cytometry following a total of 48 h of the incubation as described above. In blocking experiments using the RGD peptide, human $CD34^+$ cells and K562 cells were preincubated in the medium containing synthetic RGD peptide (GRGDSP, GRGESP; TaKaRa, Osaka, Japan) at 4 °C for 1 h. Subsequently, the cells were transduced with Ad35GFP at 3000 VP per cell for 3 h ($CD34^+$ cells) or 1000 VP per cell for 1 h (K562 cells) at 37 °C after which the cells were washed, resuspended in a fresh medium and incubated at 37 °C GFP expression levels were measured 48 h after transduction as described above. Blocking experiments were similarly performed using monoclonal anti-human integrin antibodies. Following incubation with anti-human integrin antibodies (50 μg ml^{-1}), the cells were transduced with Ad35GFP at 3000 VP per cell for 3 h ($CD34^+$ cells) or 300 VP per cell for 0.5 h (K562 cells). GFP expression levels were evaluated as described above.

Cellular binding and uptake of Ad35 vectors

For evaluation of effects of divalent cations on cellular binding and uptake of Ad35 vectors, K562 cells, which were seeded at 3×10^4 cells $well^{-1}$ into a 48-well plate, were incubated with Ad35GFP in the presence of 5 mM EDTA or Mn^{2+} for 1.5 h at 4 or 37 °C as described above. The cells were then recovered and washed five times with ice-cold phosphate-buffered saline, and total DNA, including the Ad vector DNA, was extracted from the cells using DNeasy Tissue Kit (Qiagen). Quantitative real-time PCR was performed as described previously.[23] In transduction-blocking experiments using the RGD peptide, human $CD34^+$ cells and K562 cells were incubated with Ad35GFP at 4 or 37 °C in the presence of 200 μg ml^{-1} of the RGD peptide for 3 h ($CD34^+$ cells) or 1.5 h (K562 cells) as described above. Following incubation, the cells were washed and the vector genome numbers were measured by real-time PCR analysis, as described above. The amounts of vector genome of Ad35GFP, Ad35RGE-GFP and Ad35ΔRGD-GFP were similarly evaluated following incubation with Ad35GFP, Ad35RGE-GFP and Ad35ΔRGD-GFP at 6000 VP per cell for 3 h ($CD34^+$ cells) or 3000 VP per cell for 1.5 h (K562 cells) at 4 or 37 °C.

Acknowledgements

We thank Ms Kimiyo Akitomo for her technical assistance. This work was supported by grants for Health and Labour Sciences Research from the Ministry of Health, Labour and Welfare of Japan.

References

1 Shenk T. Adenoviridae. In: Knipe DM, Howley PM (eds). *Fields Virology*. Lippincott Williams and Wilkins: Philadelphia, 2001, pp 2265–2301.
2 Li E, Brown SL, Stupack DG, Puente XS, Cheresh DA, Nemerow GR. Integrin alpha(v)beta1 is an adenovirus coreceptor. *J Virol* 2001; **75**: 5405–5409.
3 Wickham TJ, Mathias P, Cheresh DA, Nemerow GR. Integrins alpha v beta 3 and alpha v beta 5 promote adenovirus internalization but not virus attachment. *Cell* 1993; **73**: 309–319.
4 Wickham TJ, Filardo EJ, Cheresh DA, Nemerow GR. Integrin alpha v beta 5 selectively promotes adenovirus mediated cell membrane permeabilization. *J Cell Biol* 1994; **127**: 257–264.
5 Davison E, Diaz RM, Hart IR, Santis G, Marshall JF. Integrin alpha5beta1-mediated adenovirus infection is enhanced by the integrin-activating antibody TS2/16. *J Virol* 1997; **71**: 6204–6207.
6 Huang S, Kamata T, Takada Y, Ruggeri ZM, Nemerow GR. Adenovirus interaction with distinct integrins mediates separate events in cell entry and gene delivery to hematopoietic cells. *J Virol* 1996; **70**: 4502–4508.
7 Rebel VI, Hartnett S, Denham J, Chan M, Finberg R, Sieff CA. Maturation and lineage-specific expression of the coxsackie and adenovirus receptor in hematopoietic cells. *Stem Cells* 2000; **18**: 176–182.
8 Tillman BW, de Gruijl TD, Luykx-de Bakker SA, Scheper RJ, Pinedo HM, Curiel TJ *et al*. Maturation of dendritic cells accompanies high-efficiency gene transfer by a CD40-targeted adenoviral vector. *J Immunol* 1999; **162**: 6378–6383.
9 Hemminki A, Kanerva A, Liu B, Wang M, Alvarez RD, Siegal GP *et al*. Modulation of coxsackie-adenovirus receptor expression for increased adenoviral transgene expression. *Cancer Res* 2003; **63**: 847–853.
10 Bauerschmitz GJ, Barker SD, Hemminki A. Adenoviral gene therapy for cancer: from vectors to targeted and replication competent agents (review). *Int J Oncol* 2002; **21**: 1161–1174.
11 Gaggar A, Shayakhmetov DM, Lieber A. CD46 is a cellular receptor for group B adenoviruses. *Nat Med* 2003; **9**: 1408–1412.
12 Segerman A, Atkinson JP, Marttila M, Dennerquist V, Wadell G, Arnberg N. Adenovirus type 11 uses CD46 as a cellular receptor. *J Virol* 2003; **77**: 9183–9191.
13 Segerman A, Mei YF, Wadell G. Adenovirus types 11p and 35p show high binding efficiencies for committed hematopoietic cell lines and are infective to these cell lines. *J Virol* 2000; **74**: 1457–1467.
14 Mei YF, Segerman A, Lindman K, Hornsten P, Wahlin A, Wadell G. Human hematopoietic (CD34+) stem cells possess high-affinity receptors for adenovirus type 11p. *Virology* 2004; **328**: 198–207.
15 Sakurai F, Mizuguchi H, Hayakawa T. Efficient gene transfer into human CD34+ cells by an adenovirus type 35 vector. *Gene Therapy* 2003; **10**: 1041–1048.
16 Sakurai F, Murakami S, Kawabata K, Okada N, Yamamoto A, Seya T *et al*. The short consensus repeats 1 and 2, not the cytoplasmic domain, of human CD46 are crucial for infection of subgroup B adenovirus serotype 35. *J Control Release* 2006; **113**: 271–278.
17 Persson BD, Reiter DM, Marttila M, Mei YF, Casasnovas JM, Arnberg N *et al*. Adenovirus type 11 binding alters the

conformation of its receptor CD46. *Nat Struct Mol Biol* 2007; **14**: 164–166.
18 Fleischli C, Verhaagh S, Havenga M, Sirena D, Schaffner W, Cattaneo R *et al*. The distal short consensus repeats 1 and 2 of the membrane cofactor protein CD46 and their distance from the cell membrane determine productive entry of species B adenovirus serotype 35. *J Virol* 2005; **79**: 10013–10022.
19 Mathias P, Wickham T, Moore M, Nemerow G. Multiple adenovirus serotypes use alpha v integrins for infection. *J Virol* 1994; **68**: 6811–6814.
20 Zubieta C, Schoehn G, Chroboczek J, Cusack S. The structure of the human adenovirus 2 penton. *Mol Cell* 2005; **17**: 121–135.
21 Albinsson B, Kidd AH. Adenovirus type 41 lacks an RGD alpha(v)-integrin binding motif on the penton base and undergoes delayed uptake in A549 cells. *Virus Res* 1999; **64**: 125–136.
22 Lozahic S, Christiansen D, Manie S, Gerlier D, Billard M, Boucheix C *et al*. CD46 (membrane cofactor protein) associates with multiple beta1 integrins and tetraspans. *Eur J Immunol* 2000; **30**: 900–907.
23 Sakurai F, Kawabata K, Yamaguchi T, Hayakawa T, Mizuguchi H. Optimization of adenovirus serotype 35 vectors for efficient transduction in human hematopoietic progenitors: comparison of promoter activities. *Gene Therapy* 2005; **12**: 1424–1433.
24 Sakurai F, Mizuguchi H, Yamaguchi T, Hayakawa T. Characterization of *in vitro* and *in vivo* gene transfer properties of adenovirus serotype 35 vector. *Mol Ther* 2003; **8**: 813–821.
25 Leitinger B, McDowall A, Stanley P, Hogg N. The regulation of integrin function by Ca(2+). *Biochim Biophys Acta* 2000; **1498**: 91–98.
26 Mould AP, Garratt AN, Askari JA, Akiyama SK, Humphries MJ. Regulation of integrin alpha 5 beta 1 function by anti-integrin antibodies and divalent cations. *Biochem Soc Trans* 1995; **23**: 395S.
27 Solovjov DA, Pluskota E, Plow EF. Distinct roles for the alpha and beta subunits in the functions of integrin alphaMbeta2. *J Biol Chem* 2005; **280**: 1336–1345.
28 Meier O, Greber UF. Adenovirus endocytosis. *J Gene Med* 2003; 5: 451–462.
29 Wu E, Pache L, Von Seggern DJ, Mullen TM, Mikyas Y, Stewart PL *et al*. Flexibility of the adenovirus fiber is required for efficient receptor interaction. *J Virol* 2003; **77**: 7225–7235.
30 Shayakhmetov DM, Papayannopoulou T, Stamatoyannopoulos G, Lieber A. Efficient gene transfer into human CD34(+) cells by a retargeted adenovirus vector. *J Virol* 2000; **74**: 2567–2583.
31 Saban SD, Nepomuceno RR, Gritton LD, Nemerow GR, Stewart PL. CryoEM structure at 9A resolution of an adenovirus vector targeted to hematopoietic cells. *J Mol Biol* 2005; **349**: 526–537.
32 Segerman A, Arnberg N, Erikson A, Lindman K, Wadell G. There are two different species B adenovirus receptors: sBAR, common to species B1 and B2 adenoviruses, and sB2AR, exclusively used by species B2 adenoviruses. *J Virol* 2003; **77**: 1157–1162.
33 Tuve S, Wang H, Ware C, Liu Y, Gaggar A, Bernt K *et al*. A new group B adenovirus receptor is expressed at high levels on human stem and tumor cells. *J Virol* 2006; **80**: 12109–12120.
34 Teuchert M, Maisner A, Herrler G. Importance of the carboxyl-terminal FTSL motif of membrane cofactor protein for basolateral sorting and endocytosis. Positive and negative modulation by signals inside and outside the cytoplasmic tail. *J Biol Chem* 1999; **274**: 19979–19984.
35 Shayakhmetov DM, Eberly AM, Li ZY, Lieber A. Deletion of penton RGD motifs affects the efficiency of both the internalization and the endosome escape of viral particles containing adenovirus serotype 5 or 35 fiber knobs. *J Virol* 2005; **79**: 1053–1061.
36 Mizuguchi H, Koizumi N, Hosono T, Ishii-Watabe A, Uchida E, Utoguchi N *et al*. CAR- or alphav integrin-binding ablated adenovirus vectors, but not fiber-modified vectors containing RGD peptide, do not change the systemic gene transfer properties in mice. *Gene Therapy* 2002; **9**: 769–776.
37 Shayakhmetov DM, Li ZY, Ternovoi V, Gaggar A, Gharwan H, Lieber A. The interaction between the fiber knob domain and the cellular attachment receptor determines the intracellular trafficking route of adenoviruses. *J Virol* 2003; **77**: 3712–3723.
38 Pierschbacher MD, Ruoslahti E. Influence of stereochemistry of the sequence Arg-Gly-Asp-Xaa on binding specificity in cell adhesion. *J Biol Chem* 1987; **262**: 17294–17298.
39 Mizuguchi H, Kay MA. A simple method for constructing E1- and E1/E4-deleted recombinant adenoviral vectors. *Hum Gene Ther* 1999; **10**: 2013–2017.
40 Mizuguchi H, Kay MA. Efficient construction of a recombinant adenovirus vector by an improved *in vitro* ligation method. *Hum Gene Ther* 1998; **9**: 2577–2583.
41 Kawabata K, Sakurai F, Yamaguchi T, Hayakawa T, Mizuguchi H. Efficient gene transfer into mouse embryonic stem cells with adenovirus vectors. *Mol Ther* 2005; **12**: 547–554.
42 Sakurai F, Kawabata K, Koizumi N, Inoue N, Okabe M, Yamaguchi T *et al*. Adenovirus serotype 35 vector-mediated transduction into human CD46-transgenic mice. *Gene Therapy* 2006; **13**: 1118–1126.
43 Maizel Jr JV, White DO, Scharff MD. The polypeptides of adenovirus. I. Evidence for multiple protein components in the virion and a comparison of types 2, 7A, and 12. *Virology* 1968; **36**: 115–125.

Genes and Environment, Vol. 29, No. 3 pp. 115–127 (2007)

Regular article

Differential Gene Expression Induced by Two Genotoxic *N*-nitroso Carcinogens, Phenobarbital and Ethanol in Mouse Liver Examined with Oligonucleotide Microarray and Quantitative Real-time PCR[1]

Takashi Watanabe[2], Kaori Tobe[2], Yutaka Nakachi[3], Yasumitsu Kondoh[3], Madoka Nakajima[4], Shuichi Hamada[5], Chiaki Namiki[6], Takayoshi Suzuki[7], Satoru Maeda[2], Ayami Tadakuma[2], Mikiya Sakurai[2], Yuko Arai[2], Atsushi Hyogo[8], Masako Hoshino[9], Tomoko Tashiro[2], Hisashi Ito[2], Hiroshige Inazumi[9], Yoshiyuki Sakaki[10], Hideo Tashiro[3] and Chie Furihata[1,11]

[2]Department of Chemistry and Biological Science, and [9]Department of Information Technology, School of Science and Engineering, Aoyama Gakuin University, Kanagawa Japan, [3]Advanced Engineering Center, RIKEN, Japan, [4]Genetic Toxicology Group, Biosafety Research Center, Foods, Drugs, and Pesticides, Shizuoka, Japan, [5]Genetic Toxicology Group, Toxicology Division II, Kashima Laboratory, Mitsubishi Chemical Safety Institute LTD., Japan, [6]Central Research Laboratory, SSP Co. Ltd., Chiba, Japan, [7]Division of Cellular & Gene Therapy Products, National Institute of Health Sciences, Tokyo, Japan, [8]Laboratory Animal Science and Toxicology Laboratories, Sankyo Co. Ltd., Shizuoka, Japan, [10]Genetic Sciences Center, RIKEN, Kanagawa, Japan

(Received December 7, 2006; Revised April 17, 2007, June 25, 2007; Accepted June 27, 2007)

It is known that genotoxic *N*-nitroso carcinogens induce DNA damage in mouse liver within a few hours and induce mutations within 28 days after their administration. However, related-gene expression changes at these time points in liver were not fully elucidated. Differential gene expression induced by two genotoxic *N*-nitroso carcinogens in mouse liver was examined 4 h and 28 days after their administration with in-house oligonucleotide microarray (268 genes) and quantitative real-time PCR, and compared to that of a non-genotoxic carcinogen and a non-carcinogenic toxin. Diethylnitrosamine (DEN, 80 mg/kg bw), dipropylnitrosamine (DPN, 250 mg/kg bw), phenobarbital sodium (30 mg/kg bw) and ethanol (1000 mg/kg bw) were injected intraperitoneally into groups of male 9-week-old B6C3F1 mice and liver was dissected after 4 h and 28 days. mRNA from pooled livers was reverse-transcribed to cDNA, and Cy3- and Cy5-labeled cDNA was competitively hybridized with in-house made microarray, scanned and analyzed; additionally, quantitative real-time PCR was performed for selected genes. Differential gene expression between two genotoxic *N*-nitroso carcinogens and phenobarbital and ethanol was observed in 11 genes 4 h after administration, including seven tumor suppressor *p53* target genes, viz. *c-Jun*, *Ccng1*, *Mdm2*, *p21*, *Bax*, *Hsp27* and *Snk*; the other genes were *Mbd1*, *Hmox-1*, *Ccnf* and *Rad52*. However, only some degree of differential gene expression of *p21*, *Ccng1* and *Snk* was observed 28 days after administration; no other differentially-expressed genes were evident. The present results suggest that DEN and DPN induce differential gene expression in *p53* target genes in liver within a few hours after administration and that these acute responses remained only partially in liver after 28 days.

Key words: quantitative real-time PCR, oligonucleotide microarray, toxicogenomics, genotoxic carcinogens, non-genotoxic tumor promoter

Introduction

Toxicogenomics is a rapidly developing discipline to aid understanding the molecular and cellular effects of chemicals in biological systems. DNA microarray is a powerful technology for characterizing gene expression on a genome scale (1), although issues of reliability, reproducibility and correlation of data produced across the different DNA microarrays are still being addressed (2). There are several commercially available microar-

[1]This work was partly a JEMS/MMS/Toxicogenomics group collaborative study (C. Furihata, T. Watanabe, M. Nakajima, S. Hamada, C. Namiki, T. Suzuki and A. Hyogo).

[11]Correapondence to: Chie Furihata, Department of Chemistry and Biological Science, School of Science and Engineering, Aoyama Gakuin University, 5-10-1 Fuchinobe, Sagamihara, Kanagawa 229-8558, Japan. Tel: +81-42-759-6233, Fax: +81-42-759-6511, E-mail: chiefurihata@gmail.com

rays (3–5) but which are very expensive and time-consuming. It may therefore be economical to prepare in-house microarray that contains a small number of selected genes for a specific purpose and which is easy to analyze. We tried preparing in-house oligonucleotide microarray useful for characterizing mutagenic and carcinogenic chemicals and for differentiating from non-genotoxic carcinogens and non-carcinogenic toxic compounds, and applied it to the study of early response in mouse liver in order to clarify key word genes and to develop chemical risk assessment microarray. Quantitative real-time PCR (qPCR) is an alternative technology for toxicogenomics (6). qPCR is thought to be a reliable quantitative method but takes time to analyze a large number of genes. DNA microarray and qPCR would be complementary to each other.

It is known that genotoxic *N*-nitroso carcinogens induce DNA damage and repair in mouse liver in a matter of a few hours after their administration; DNA adducts (7), unscheduled DNA synthesis (8), DNA lesions (Comet assay) (9) and other lesions have been reported. It is also known that mutations are induced in transgenic mouse liver 28 days after genotoxic *N*-nitroso carcinogen administration (7,10,11). This coincides with the time at which chronic changes leading to carcinogenesis are known to begin. However, related-gene expression changes at these time points are not yet fully elucidated.

We compared gene expression profiles after mouse liver exposure to typical carcinogenic *N*-nitroso compounds (diethylnitrosamine and dipropylnitrosamine), to a non-genotoxic carcinogen (phenobarbital) and to a non-carcinogenic liver toxin (ethanol). This is the first trial DNA microarray in our JEMS/MMS/Toxicogenomics group collaborative study. We first selected candidate genes for our in-house microarray from gene classes of DNA repair, DNA recombination, DNA methylation, DNA transcription, apoptosis, cell cycle, extracelluar matrix protein, inflammation, dendritic cell, oncogene, tumor development, tumor growth factor, tumor suppressor, xenobiotic metabolism and signal transduction, and then added genes from our preliminary results of Affymetrix GeneChip Mu74AV2. (See online supplemental Table S1 at http://www.chem.aoyama.ac.jp/Chem/ChemHP/Furihatalab/).

Materials and Methods

Animals: Eight-week-old male B6C3F1/Crj mice were purchased from Charles River Japan, Inc. (Yokohama, Japan). They were kept in plastic cages with hard wood chips as bedding in an air-conditioned room at 23±2°C and 55±5% humidity with a 12 h light/dark cycle. Food (Oriental MF, Oriental Yeast Co., Tokyo) and tap water were available *ad libitum*. All animal experiments were conducted in accordance with the NIH Guide for Care and Use of Laboratory Animals and approved by the Animal Care and Use Committee at the Biosafety Research Center, Foods, Drugs, and Pesticides.

Chemicals: Diethylnitrosamine (DEN, CAS No. 55-18-5) and dipropylnitrosamine (DPN, CAS No. 621-64-7), were purchased from Tokyo Kasei Kogyo Co., Ltd. (Tokyo, Japan). Phenobarbital sodium (PB, CAS No. 57-30-7) and ethanol (EtOH, CAS No. 64-17-5) were obtained from Wako Pure Chem. Ind. Ltd. (Osaka, Japan).

Animal experiments: Experiment I. Main lobe of liver was dissected from untreated control 9-week-old mice and immediately frozen and stored at −80°C until use for validation experiments in Fig. 1. Experiment II. Test chemicals in sterile saline were given to groups of 9-week-old mice (5 per group) intraperitoneally. Doses of chemicals were: DEN, 80 mg/kg bw, 0.2 to 0.3 mL per mouse; DPN, 250 mg/kg bw; PB, 30 mg/kg bw; EtOH, 1000 mg/kg bw. Sterile saline was injected ip into control groups of mice. Main lobe of liver was dissected after 4 h and 28 days, was pooled and immediately frozen and stored at −80°C until use for experiments in Figs. 2–4. Doses of DEN and DPN were selected that induced mutation in transgenic mice (MutaMouse or Big Blue mice) at 28 days after their administration in previous studies (10,11). The doses of PB and EtOH were half their respective LD_{50}. Experiment III. DEN and saline were given to the other groups of 9-week-old mice (5 per group) at the same dose as in experiment II. Main lobe of liver was dissected after 4 h and 28 days, was immediately frozen individually and stored at −80°C until use for individual experiment in Fig. 5.

RNA isolation: Experiment I and II. Frozen pooled main lobes of liver from 5 mice were placed directly in TRIzol reagent (Invitrogen Corp., Carlsbad, CA, USA), homogenized for 2 min on ice, and total RNA was isolated using manufacturer's protocol (12). RNA was quantified based on 260 nm absorbance reading of the solution. Quality of the RNA was assured by measuring 260 nm: 280 nm absorbance ratio and reviewing integrity on agarose denaturing gels. TRIzol reagent-isolated total RNA was additionally purified with Isogen-LS (Nippon Gene, Co. Ltd., Tokyo, Japan) (13) for real-time PCR experiments. Experiment III. Total RNA was extracted from individual mouse main lobe liver by a similar method and was examined only with qPCR.

Microarray preparation: Mounted genes (268 genes, Table S1, http://www.chem.aoyama.ac.jp/Chem/ChemHP/Furihatalab/) such as suggested genes of DNA repair, DNA recombination, DNA methylation, DNA transcription, cell cycle, apoptosis, inflammation, dendritic cell, extracelluar matrix protein,

oncogene, signal transduction, tumor development, tumor growth factor, tumor suppressor and xenobiotic metabolism were selected mainly for determining genotoxic carcinogens. 40–47mer unmodified oligonucleotide sequences for probes were determined in accordance with the National Center for Biotechnology Information (NCBI) database (http://www.ncbi.nlm.nih.gov/). Accession No. and name of genes are summarized in Table S1. Three negative control plant genes were included: [1] *A. thaliana gene* (*LHCP AB 140*) for chlorophyll a/b binding protein, [2] *Gossypium hirsutum* cellulose synthase (*celA2*) mRNA, and [3] *A. thaliana Lhb1B2* gene for photosystem II chlorophyll a binding protein. Probes were selected in 3′-end region and BLAST search (http://www.ncbi.nlm.nih.gov/) was performed respectively. Nucleotide sequences were applied to Japan Patent No. 2005-99843. 40–47mer unmodified oligonucleotides were obtained from Invitrogen (Invitrogen Japan K.K, Tokyo, Japan). Probes (50 μM) in 1×Micro Spotting Solution (ArrayIt Division, TelChem International, Inc., Sunnyvale CA, USA) and 0.2% Tween 20 were spotted on polycarbodiimide-coated slides (CarboStation-U, Nisshinbo Ind. Inc., Tokyo, Japan) with RIKEN arrayer. Spotted microarrays were rehydrated in a humid chamber with 1×SSC, UV-crosslinked (600 mJ) and washed with MilliQ water. Microarrays were stored under vacuum at 4°C.

Labeling and hybridization: Experiment I (microarray validity study): Untreated control total RNA (20 μg) was reverse-transcribed to cDNA and labeled with Alexa fluor dyes using SuperScript plus indirect cDNA labeling system with Alexa fluor dyes (Invitrogen, Corp., Carlsbad, CA, USA) in experiments in Fig. 1. Experiment II. mRNA was purified from total RNA with Oligotex-dT30 (Takara Bio Inc., Otsu, Shiga, Japan). mRNA (1 μg) of DEN, DPN, PB, EtOH and control samples (4 h and 28 days) was reverse-transcribed to cDNA and labeled with CyDye (Cy3 and Cy5) using CyScribe cDNA post labeling kit (Amersham Biosciences, Piscataway, NJ, USA) as described in manufacturer's protocol. CyDye-labeled cDNA (150 μL) was hybridized with microarray in Gene Tac Hybridization Station (Genomic Solutions, Ann Arbor, MI, USA) at 55°C overnight, washed in 2×SSC-0.1% SDS at 45°C, 1×SSC-0.1%SDS at 40°C and 0.2×SSC at 40°C, dried by centrifugation and scanned by DNAscope (Gene Focus, Waterloo, Ontario, Canada).

Data analysis of microarray results: Scanning data were analyzed using MACROview (Biomedical Photometrics Inc., Waterloo, ON, Canada) by global normalization method and further analyzed using Cluster and TreeView (http://rana.lbl.gov/EisenSoftware.htm). Gene network was analyzed using Ingenuity Pathways Analysis (Ingenuity Systems, Inc. Redwood City, CA, USA).

Table 1. qPCR primer sequences

Gene	Primer sequence
Bax 5′	gattgctgacgtggacacggac
Bax 3′	cagggccttgagcaccagtttg
Ccnf 5′	ggagctctcaagtgaagacagcac
Ccnf 3′	ggcctcacacaccattaggctac
Ccngl 5′	tggccgagatttgaccttctgg
Ccngl 3′	gtgcttcagttgccgtgcagtg
c-Jun 5′	aggcagagaggaagcgcatg
c-Jun 3′	tgtgccacctgttccctgag
Gapdh 5′	tctggaaagctgtggcgtgatg
Gapdh 3′	tcccgttcagctctgggatgac
Hmox-1 5′	gtggcctgaactttgaaaccagc
Hmox-1 3′	cgtggtcagtcaacatggatgc
Hprt 5′	cttgctcgagatgtcatgaaggag
Hprt 3′	taatccagcaggtcagcaaagaac
Hsp27 5′	ctcacagtgaagaccaaggaag
Hsp27 3′	ggatagggaagaggacactagg
Mbd1 5′	tacagccctacacgaaccagc
Mbd1 3′	gaatttgggcttgtcgcagcag
Mdm2 5′	ttgatccgagcctgggtctgtg
Mdm2 3′	aagatcctgatgcgagggcgtc
p21 5′	tccgcacaggagcaaagtgtg
p21 3′	acgcgctcccagacgaagttg
p53 5′	ttggaccctggcacctacaatg
p53 3′	gcagacaggctttgcagaatgg
Rad52 5′	gagaaccagcccaaacttctgc
Rad52 3′	gaacatgctggttggtgttgc
Snk 5′	ctgttgagagcgtcttcagttg
Snk 3′	ccatagttcacagttaagcagc

Quantitative real-time PCR (qPCR): For qPCR, 2 μL of the cDNA product solution were used to measure gene expression using DNA Engine Opticon 2 (Bio-Rad Laboratories, Inc., Hercules, CA, USA) and SYBR Green PCR Master Mix (Applied Biosystems, Foster City, CA, USA). Glyceraldehyde 3-phosphate dehydrogenase (*Gapdh*) was used as the housekeeping normalized gene for each sample. Nucleotide sequence of qPCR primers was determined in accordance with Primer3 (http://frodo.wi.mit.edu/cgi-bin/primer3/primer3_www.cgi), ncbi DNA database (http://www.ncbi.nlm.nih.gov/) and BLAST (http://www.ncbi.nlm.nih.gov/BLAST/). Primers resulted in a single product which could be visualized on a 1.2% agarose gel. Single peak of melting curve for each primer set was confirmed using DNA Engine Opticon 2. Primer sequences are summarized in Table 1. RNA (2.5 μg) was reverse-transcribed with SUPERSCRIPT First-Strand Synthesis System for RT-PCR (Invitrogen Corp., Carlsbad, CA, USA) and 250 μL cDNA product solution (12) was prepared as described in the manufacturer's protocol.

Data analysis of qPCR results: Some of the data were statistically analyzed by Student's t-test.

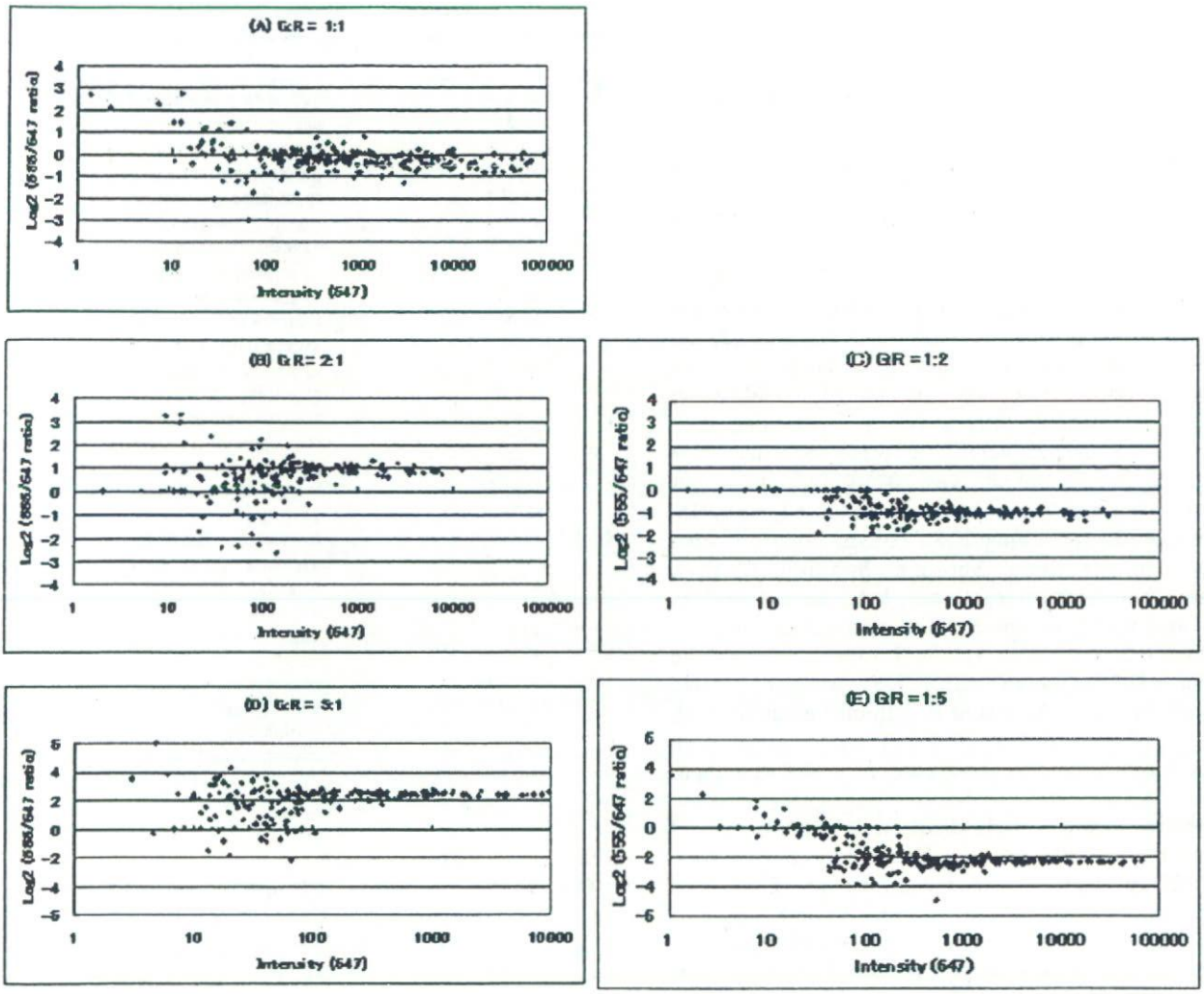

Fig. 1. The validity of the in-house made microarray expressed as Scatter pattern (Experiment I). Results of hybridization with the same control samples labeled with Alexa555 (G) and Alexa647 (R) with the ratio of Alexa555/Alexa647 of A):5/1, B):2/1, C):1/1, D):1/2 and E):1/5. Results show the expected ratio of fluorescence for each sample, demonstrating the quantitative capability of our in-house microarrays.

Results

The validity of the in-house made DNA microarray (Experiment I): Fig. 1 shows the results of hybridization with the same control cDNA samples labeled with Alexa555 (green: G) and Alexa647 (red: R) with the ratio of Alexa555/Alexa647 of 5/1, 2/1, 1/1, 1/2 and 1/5. Figs. 1A to 1E show scatter plots which reveal an equivalent ratio of fluorescence for each sample, thereby confirming the quantitative capability of our in-house DNA microarrays. Data of fluorescence intensity above 200 show good convergence which suggests high reliability in this region.

Gene expression analysis determined with DNA microarray expressed as hierarchical clustering (Experiment II): Fig. 2A shows gene expression profile in liver 4 h after administration determined with in-house DNA microarray. Only 10 differentially expressed genes and additional 3 genes are presented. Differential gene expression was observed between two genotoxic *N*-nitroso carcinogens (DEN and DPN) and PB and EtOH in 10 genes including six *p53* target genes, namely *c-Jun*, *Ccng1*, *Mdm2*, *Bax*, *Snk* and *Hsp27*; the other differentially expressed genes were *Mbd1*, *Hmox-1*, *Ccnf*, and *Rad52*. Gene expression changes were very similar for DEN and DPN. However, differential gene expression of *p53* itself was not observed 4 h after treatment in the present experimental conditions. *Gapdh* and *Hprt*, house-keeping genes, did not change their expressions 4 h after administration. Specific expression-changed genes for PB or EtOH were not found in the present 268 gene-list.

Fig. 2B shows gene expression profile for the same 13

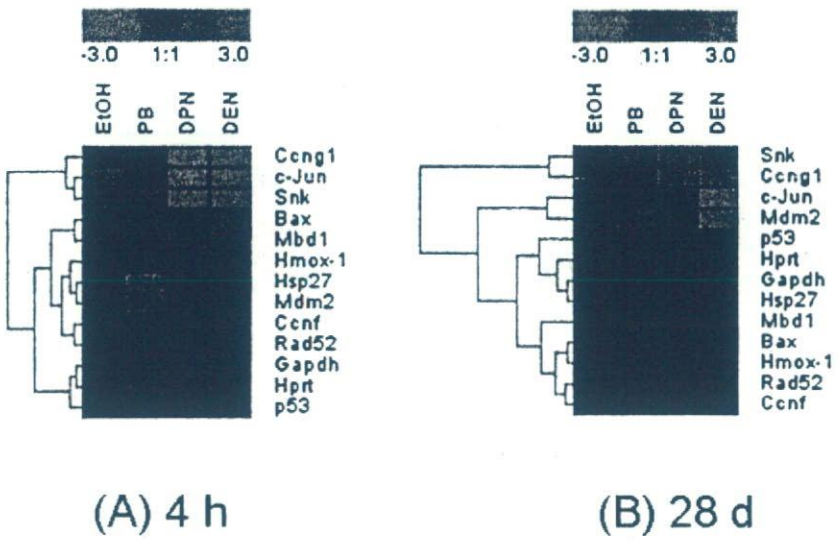

Fig. 2. Gene expression analysis determined with DNA microarray expressed as hierarchical clustering (Experiment II). Eleven differentially expressed genes and 3 expression-unchanged genes are presented. A): at 4 h, B): at 28 days. Livers were from B6C3F1 mice treated with DEN, DPN, PB or EtOH for 4 h and 28 days. Genes are listed in rows, and chemicals are listed in columns. The ratio of gene expression levels (experiment group/control group) is color coded. Green indicates down-regulation, black means no change, and red indicates up-regulation of expression. Color shows gradation of −3 or less (decrease, green) to 1 (black) to 3 or more (increase, red), as log2 expression. *Gapdh* and *Hprt* are house-keeping genes.

genes in liver 28 days after administration determined with in-house DNA microarray. There was a small degree of differential gene expression of *Ccng1* and *Snk* observed at 28 days. Expression of other genes returned to control level at 28 days after administration of DEN and DPN, and there were no newly-appeared differentially expressed genes by DEN and DPN at this time. PB and EtOH did not show significant increase or decrease of gene expression 28 days after administration in these 13 genes examined with DNA microarray. *Gapdh* and *Hprt*, house-keeping genes, did not change their expressions 28 days after administration. Specific expression-changed genes for PB or EtOH at that time point were not found in the present 268 gene-list.

Verification of DNA microarray results with qPCR (Experiment II): Figs. 3A to 3O show qPCR verification of DNA microarray results (Fig. 2A) of 10 expression-changed genes and three expression-unchanged genes 4 h after chemical administration. Differential gene expression was observed with qPCR between two genotoxic *N*-nitroso carcinogens (DEN and DPN) and PB and EtOH in 10 genes including six *p53* target genes. Generally, qPCR results coincided with DNA microarray results for these genes, suggesting considerable reliability of our DNA microarray results. An important *p53* target gene, *p21*, was additionally examined with qPCR, and a very large increase in *p21* expression (120-fold) for DEN was observed with qPCR. Relative expression (experiment group/control group) of 11 expression-changed genes was generally in some degree greater with DEN than with DPN.

Figs. 4A to 4O show qPCR verification of DNA microarray results (Fig. 2B) of the same 13 genes 28 days after chemical administration. Generally, qPCR results coincided with DNA microarray results for these genes, suggesting considerable reliability of our DNA microarray results. While there was a small degree of differential gene expression of *Ccng1* and *Snk* observed at 28 days, distinctive differences between *N*-nitroso carcinogenic compounds and PB and EtOH were not observed in the other 8 genes that were differentially expressed at 4 h after administration. *p21* was additionally examined with qPCR, and differential gene expression of *p21* was observed between *N*-nitroso carcinogenic compounds and PB and EtOH, but the increase was about 1/10 of that at 4 h (Fig. 4O vs. Fig. 3O). *Gapdh* and *Hprt*, house-keeping genes, did not change their expressions 28 days after administration. Specific expression-changed genes for PB or EtOH were not found in the present 268 gene-list.

Variation among individuals determined with qPCR (Experiment III): Fig. 5 (individual results) and Table 2 (mean ± SD) show individual relative expression of 5 genes presented in Fig. 3 and Fig. 4. Figs. 5A and 5B show relative expression of *Gapdh* in samples of 5 control-4 h, DEN-4 h, control-28 d and DEN-28 d individual livers determined with qPCR. This reveals that *Gapdh* expression was similar in each liver, i.e. variation among individuals was small, and that cDNA preparation was appropriate. In subsequent experi-

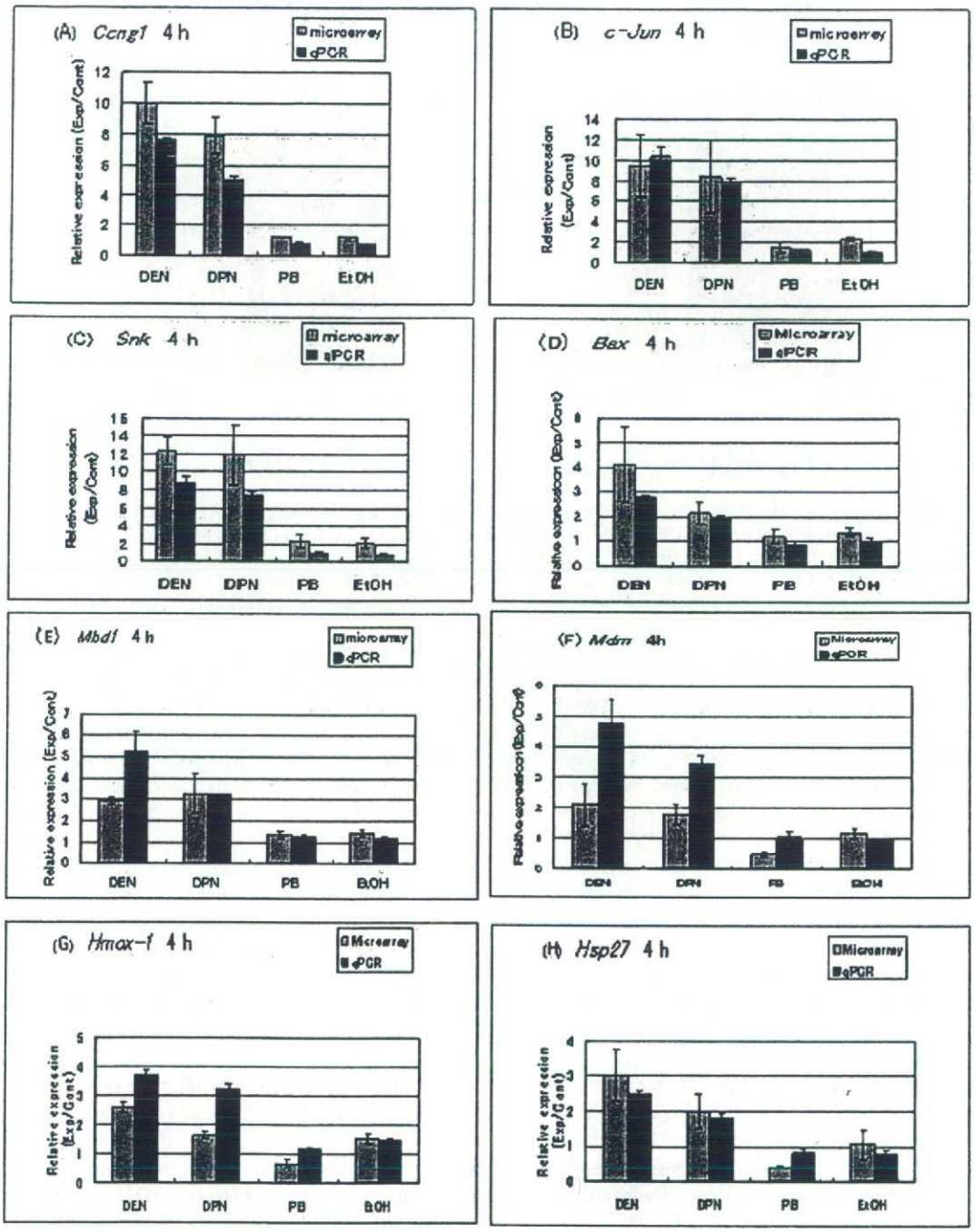

Fig. 3.

ments, *Gapdh* was used as the house-keeping normalized gene for each sample. Figs. 5C to 5J show relative gene expression of *c-Jun, Ccng1, Hsp27* and *Rad52* normalized to *Gapdh*. Variation among individual gene expression of *c-Jun, Ccng1, Hsp27* and *Rad52* (Fig. 5C to 5J) was small. Increase in gene expression by DEN at 4 h was 12-fold for *c-Jun*, 6-fold *Ccng1*, and around 2-fold for *Hsp27* and *Rad52*. In the main, these increases returned to about control level 28 days after DEN administration; *Ccng1* was slightly elevated over control at this time point. These results show that there was minor variation in the gene expression in individual livers for the various treatment groups.

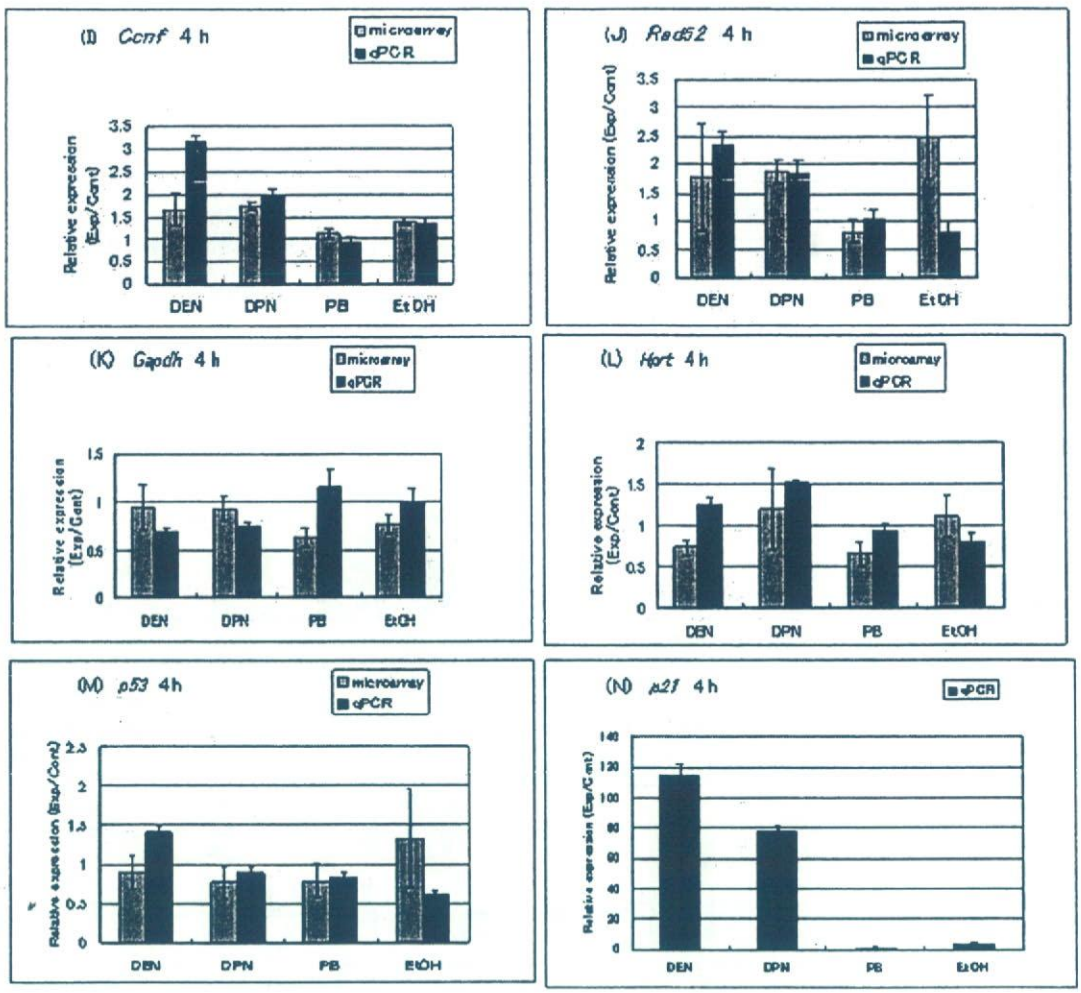

Fig. 3. Verification of DNA microarray results with qPCR 4 h after chemical administration (Experiment II). Results are shown as average and SD (error bar), and expressed as relative expression (experiment group/vehicle control group). Microarray: data are from 4 spots from two microarrays for DEN and DPN, and from 4 spots from one microarray for PB and EtOH. qPCR: results from triplicate assays. mRNA or total RNA from pooled livers from 5 mice was used as material. Only qPCR result is shown for *p21*.

Discussion

In the present study we examined differential gene expression in mouse liver 4 h and 28 days after administration of genotoxic *N*-nitroso carcinogens, DEN and DPN, compared to non-genotoxic carcinogen PB and non-carcinogenic toxin EtOH using in-house DNA microarray and qPCR. Four hours is a time at which genotoxic *N*-nitroso carcinogens induce DNA damage (7–9). We found differential gene expression between the two *N*-nitroso carcinogens and PB and EtOH in 11 genes 4 h after administration. The most characteristic genes were seven *p53* (14) target genes, viz. *c-Jun* (*c-jun* proto oncogene) (15), *Ccng1* (cyclin G1) (16), *Mdm2* (transformed 3T3 cell double minute 2, *p53* binding protein) (17), *p21* (cyclin-dependent kinase inhibitor 1A) (18), *Bax* (*Bcl2*-associated X protein) (19), *Hsp27* (heat shock protein HSP27) (20) and *Snk* (serum-inducible protein kinase) (21). A suggested gene network is shown in Fig. 6. There are about 40 DEN- and DPN-related direct or indirect *p53* target genes in the 268 gene-list analyzed using Ingenuity Pathways Analysis. Results of differentially expressed genes are presented in this manuscript.

These *p53* target genes may lead to either DNA repair or apoptosis according to the seriousness of DNA damage by DEN and DPN. However, changes in gene expression of *p53* itself were not observed in the present experimental conditions. It might be possible that this "chief protector" *p53* gene is always expressed adequately in mouse liver to function against DNA damaging hazards. Another possibility might be that *p53* expression changed earlier than 4 h and returned to

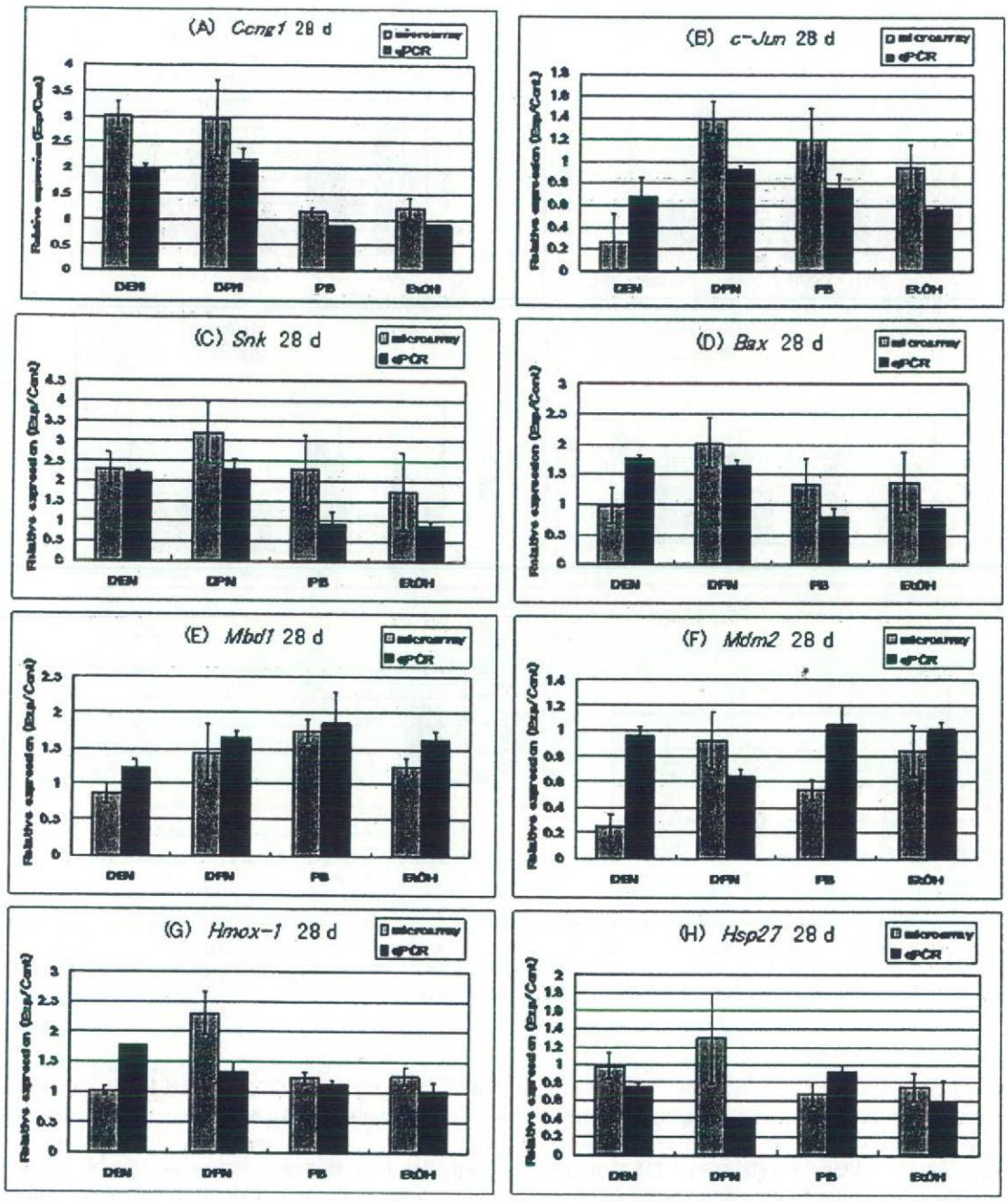

Fig. 4.

control level by 4 h. Differential gene expression of DNA repair enzymes was not detected, against expectations. DNA damage in liver by PB or EtOH at 4 h after their administration has not been reported.

Regarding differential gene expression in mouse liver 28 days after chemical exposure, it was previously reported that few DNA adducts were observed at this time after DEN administration but that mutations were observed (7). Our results showed that *p21* retained high gene expression but was reduced to one-tenth compared to 4 h, and that *Ccng1* and *Snk* showed minor increase in gene expression 28 days after administration of DEN and DPN. Expression of other genes which had elevated expression at 4 h returned to control level 28 days after administration of DEN and DPN. Differential expression of all other genes in the 268 gene-list examined did

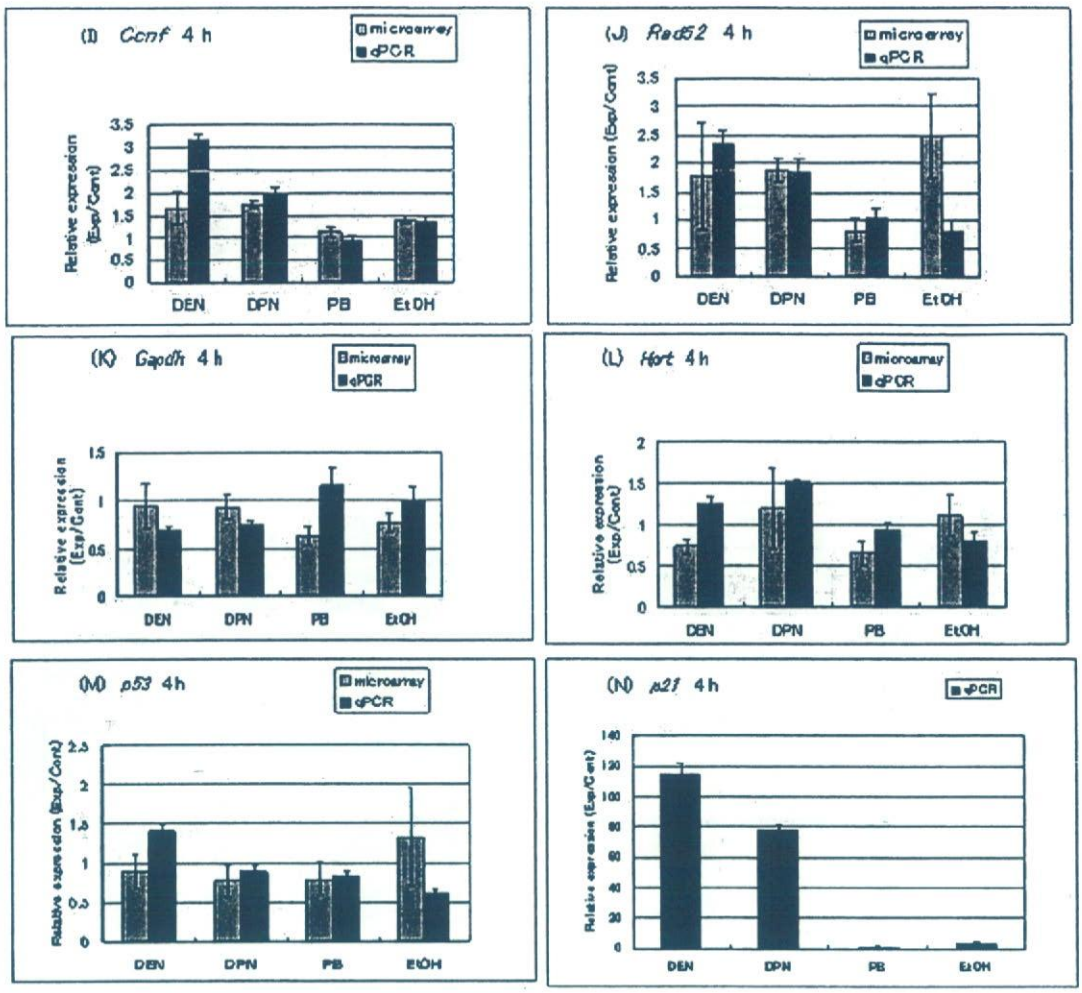

Fig. 3. Verification of DNA microarray results with qPCR 4 h after chemical administration (Experiment II). Results are shown as average and SD (error bar), and expressed as relative expression (experiment group/vehicle control group). Microarray: data are from 4 spots from two microarrays for DEN and DPN, and from 4 spots from one microarray for PB and EtOH. qPCR: results from triplicate assays. mRNA or total RNA from pooled livers from 5 mice was used as material. Only qPCR result is shown for *p21*.

Discussion

In the present study we examined differential gene expression in mouse liver 4 h and 28 days after administration of genotoxic *N*-nitroso carcinogens, DEN and DPN, compared to non-genotoxic carcinogen PB and non-carcinogenic toxin EtOH using in-house DNA microarray and qPCR. Four hours is a time at which genotoxic *N*-nitroso carcinogens induce DNA damage (7-9). We found differential gene expression between the two *N*-nitroso carcinogens and PB and EtOH in 11 genes 4 h after administration. The most characteristic genes were seven *p53* (14) target genes, viz. *c-Jun* (*c-jun* proto oncogene) (15), *Ccng1* (cyclin G1) (16), *Mdm2* (transformed 3T3 cell double minute 2, *p53* binding protein) (17), *p21* (cyclin-dependent kinase inhibitor 1A) (18), *Bax* (*Bcl2*-associated X protein) (19), *Hsp27* (heat shock protein HSP27) (20) and *Snk* (serum-inducible protein kinase) (21). A suggested gene network is shown in Fig. 6. There are about 40 DEN- and DPN-related direct or indirect *p53* target genes in the 268 gene-list analyzed using Ingenuity Pathways Analysis. Results of differentially expressed genes are presented in this manuscript.

These *p53* target genes may lead to either DNA repair or apoptosis according to the seriousness of DNA damage by DEN and DPN. However, changes in gene expression of *p53* itself were not observed in the present experimental conditions. It might be possible that this "chief protector" *p53* gene is always expressed adequately in mouse liver to function against DNA damaging hazards. Another possibility might be that *p53* expression changed earlier than 4 h and returned to

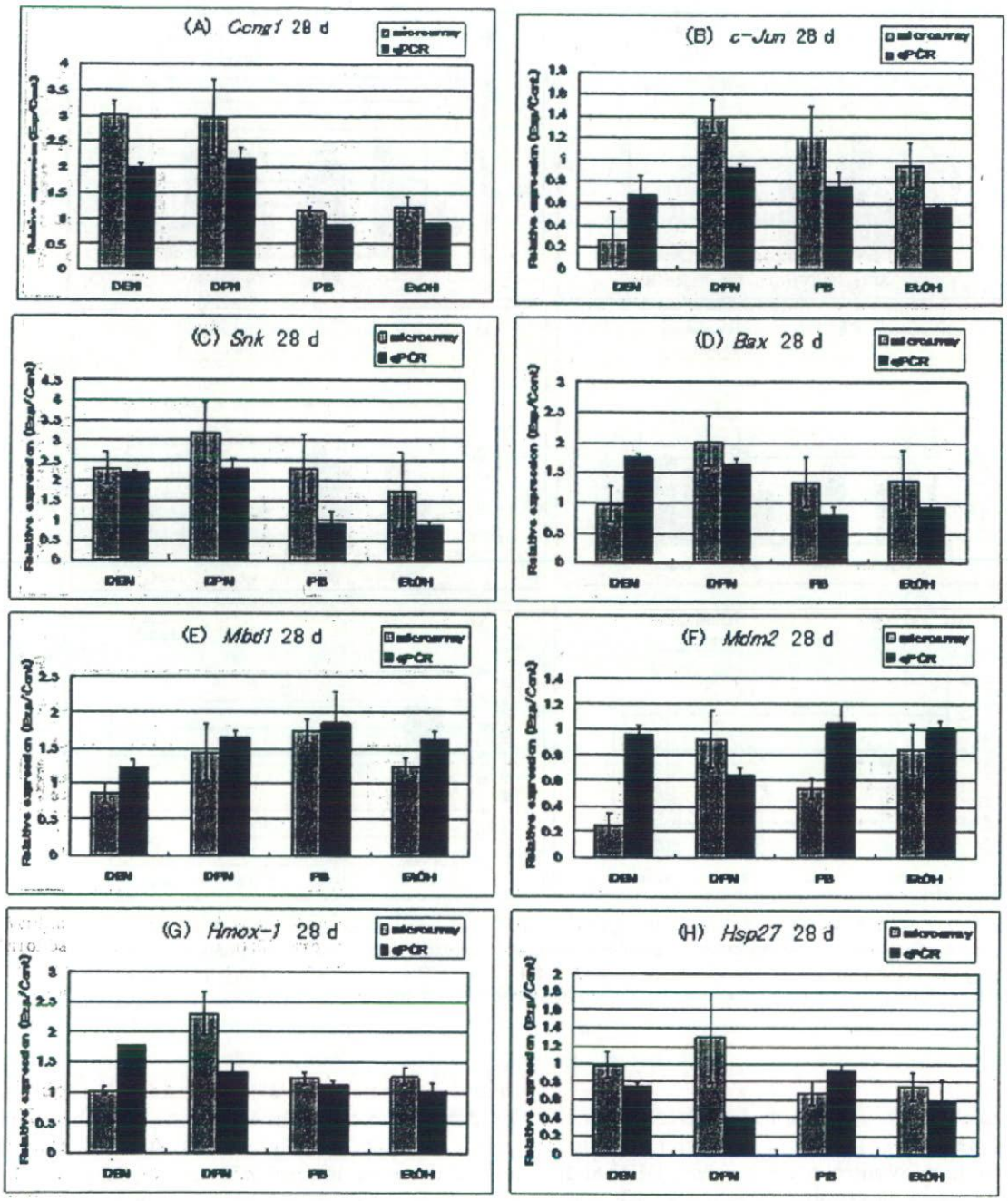

Fig. 4.

control level by 4 h. Differential gene expression of DNA repair enzymes was not detected, against expectations. DNA damage in liver by PB or EtOH at 4 h after their administration has not been reported.

Regarding differential gene expression in mouse liver 28 days after chemical exposure, it was previously reported that few DNA adducts were observed at this time after DEN administration but that mutations were observed (7). Our results showed that *p21* retained high gene expression but was reduced to one-tenth compared to 4 h, and that *Ccng1* and *Snk* showed minor increase in gene expression 28 days after administration of DEN and DPN. Expression of other genes which had elevated expression at 4 h returned to control level 28 days after administration of DEN and DPN. Differential expression of all other genes in the 268 gene-list examined did

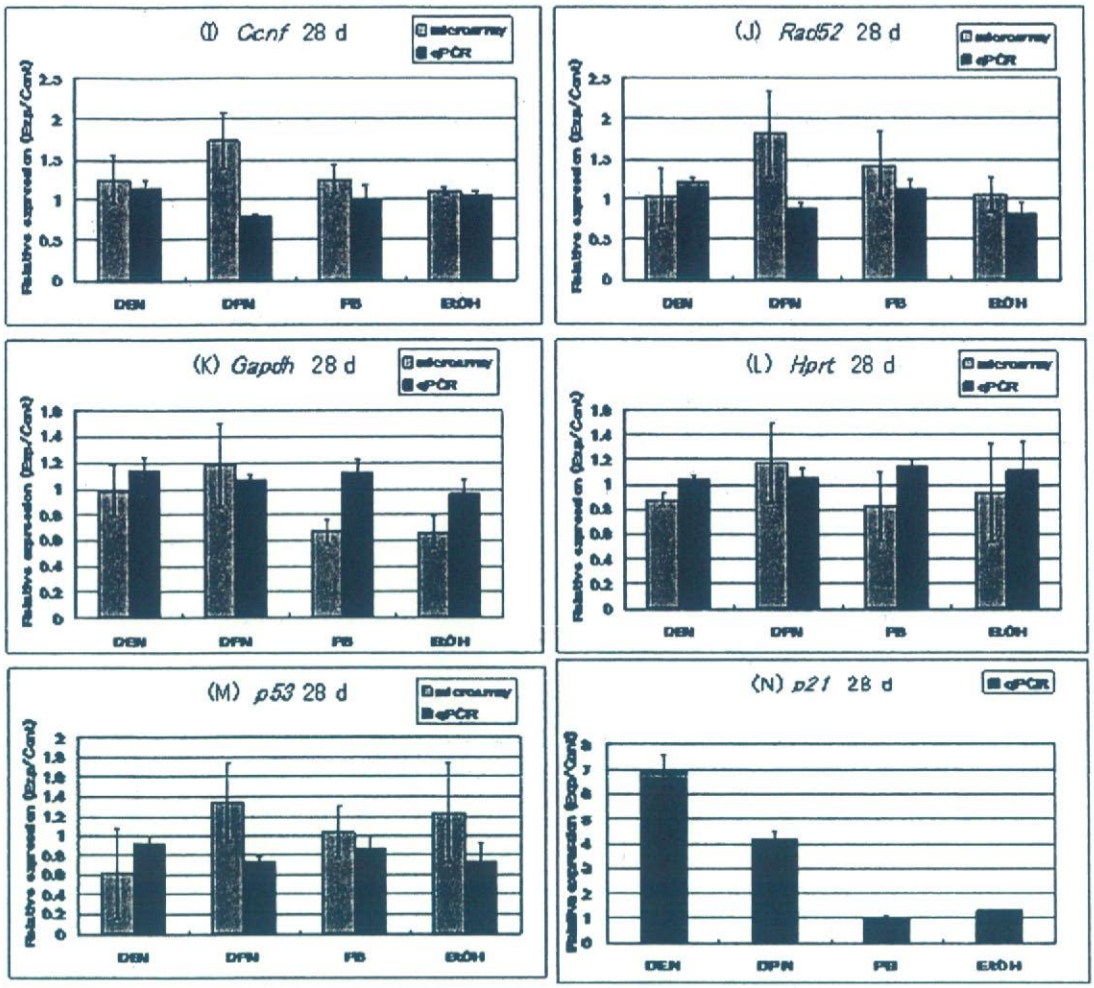

Fig. 4. Verification of DNA microarray results with qPCR 28 days after chemical administration (Experiment II). Results are shown as average and SD (error bar), and expressed as relative expression (experimental group/vehicle control group). Microarray: data are from 4 spots from two microarrays for DEN and DPN, and from 4 spots from one microarray for PB and EtOH. qPCR: results from triplicate assays. mRNA or total RNA from pooled livers from 5 mice was used as material. Only qPCR result is shown for *p21*.

not newly appear at 28 days after administration. PB and EtOH did not show significant increase or decrease of gene expression 28 days after administration. In conclusion, acute responses to the genotoxic carcinogens remained only partially in liver 28 days after administration, while PB and EtOH did not induce significant acute or longer term gene expression changes in the 268 gene-list.

Figs. 3 and 4 show that standard deviation in data sets was generally smaller in qPCR (3 tubes per experiment) than DNA microarray (4 spots per experiment). Fluorescence intensity was very similar in another experiment of the same gene (*Gapdh, Ccngl, c-Jun, Rad52, Hsp27* and others) in qPCR, indicating good reproducibility. However, fluorescence intensity in a repeat DNA microarray experiment was less reproducible, likely due to variability in fluorescent labeling of cDNA and washing of DNA microarray even if a similar amount of DNA is used for hybridization with the same lot of DNA microarray. The reliability and reproducibility of experiments are higher with qPCR than with DNA microarray in the present experimental conditions.

We demonstrated that inter-individual variation was small for all 5 genes assayed with qPCR and examined 4 h and 28 days after administration in 5 control and 5 DEN-treated mice (Fig. 5). These individual results matched well the qPCR results in Fig. 3 and Fig. 4, where liver samples of 5 different mice were pooled and assayed. Based on this, we mainly conducted experiments using pooled liver samples of 5 mice (Experiment II), although experiments using individual animal

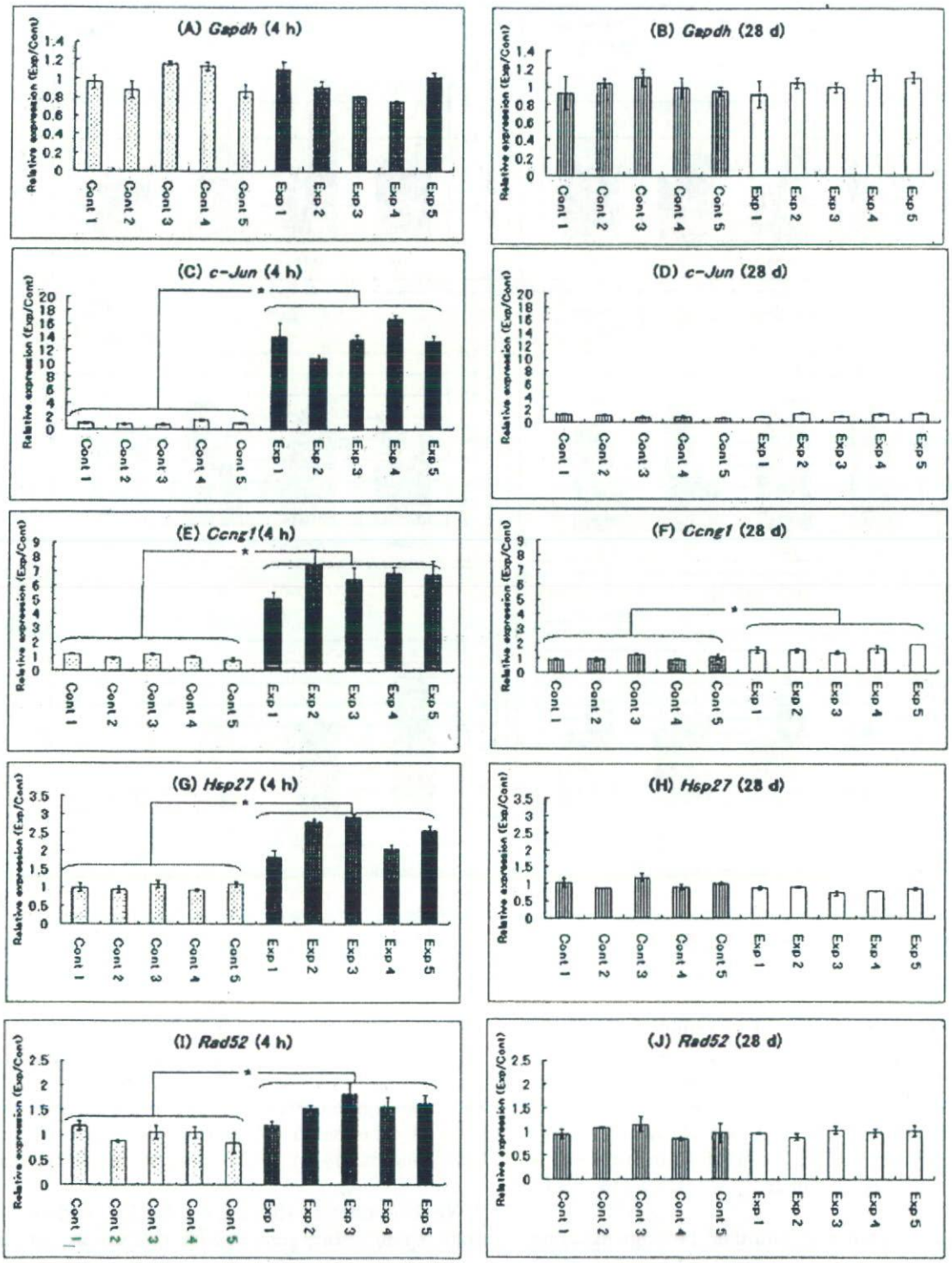

Fig. 5. Variation among individual mice (relative liver gene expression) (Experiment III). DEN (80 mg/kg bw) and saline were given to 9-week-old mice (5 per group), main lobe of liver was dissected individually after 4 h and 28 days and individual gene expression was determined with qPCR. cDNA from individual liver from 5 mice for each group was used as material. Gene expression of *Ccng1*, *c-Jun*, *Rad52* and *Hsp27* was normalized with gene expression of *Gapdh*. Values in *c-Jun* (4 h), *Ccng1* (4 h and 28 d), *Hsp27* (4 h) and *Rad53* (4 h) in DEN group were significantly different ($p < 0.01$) from control group.